Pregnancy Reduces COVID-19 Vaccine Immunity Against Novel Variants

Maclaine A. Parish[1], Jaiprasath Sachithanandham[1], Lizeth Gutierrez[2], Han-Sol Park[1], Anna Yin[1], Katerina Roznik[2], Patrick Creisher[1], John S. Lee[1], Laura A. St Clair, [1] Annie Werner[1], Catherine Pilgrim-Grayson[4], Lea Berhane[5], Hana Golding[6], Patrick Shea[1], Katherine Fenstermacher[7], Richard Rothman[7], Irina Burd[8], Jeanne Sheffield[9], Andrea L. Cox[1,2], Andrew Pekosz[1,2,7], and Sabra L. Klein[1,2*]

[1]W. Harry Feinstone Department of Molecular Microbiology and Immunology, Johns Hopkins University Bloomberg School of Public Health, Baltimore, MD, USA

[2]Department of Medicine, Division of Infectious Diseases, Johns Hopkins School of Medicine, Baltimore, MD, USA

[4] Division of Rare Diseases and Medical Genetics; Office of Rare Diseases, Pediatrics, Urologic and Reproductive Medicine; Office of New Drugs; Center for Drug Evaluation and Research; U.S. Food and Drug Administration, Silver Spring, MD, USA

[5]Division of Clinical Policy, Office of New Drug Policy, Office of New Drugs; Center for Drug Evaluation and Research; U.S. Food and Drug Administration, Silver Spring, MD, USA

[6]Division of Viral Products, Center of Biologics Evaluation and Research, U.S. Food and Drug Administration, Silver Spring, MD, USA

[7]Department of Emergency Medicine, Johns Hopkins School of Medicine, Baltimore, MD, USA

[8]Department of Obstetrics, Gynecology and Reproductive Sciences, University of Maryland School of Medicine, Baltimore, MD, USA

[9]Department of Obstetrics and Gynecology, Johns Hopkins School of Medicine, Baltimore, MD, USA

*Address correspondence to Sabra L. Klein, (410)955-8898, sklein2@jhu.edu

Abstract

Pregnant women are at heightened risk for severe outcomes from many infectious diseases, including COVID-19. Pregnant women were not included in the initial COVID-19 vaccine clinical trials which might have contributed to low rates of vaccine uptake among them (15% or lower). We explored the serological and cellular responses to COVID-19 mRNA booster vaccines (i.e., ancestral and BA.5) in pregnant and age-matched, non-pregnant females to identify how pregnancy affects immunity against vaccine viruses in addition to novel variants. Blood was collected from participants prior to and 3-5 weeks post booster vaccine. Post-vaccination antibodies from pregnant women were less cross-reactive to non-vaccine antigens, including XBB1.5 and JN.1, than antibodies from non-pregnant females. Antibodies from non-pregnant females showed strong correlations between IgG1 and FcR binding and greater IgG1:IgG3 ratios and live-virus neutralization against all variants. In contrast, antibodies from pregnant women had lower IgG1:IgG3 ratios and neutralization and greater antibody-dependent NK cell cytokine production and neutrophil phagocytosis, particularly against variants. CD4+ T cells from pregnant patients exhibited reduced polyfunctionality, with IFNγ+ monofunctional dominance. In contrast, among non-pregnant women, CD4+ T cells displayed greater polyfunctionality, with more IL-21+ cells. Pregnancy may reduce the breadth, composition, and magnitude of humoral and cellular immunity, particularly in response to novel variants.

45 **Introduction**

46 Pregnant women faced significant morbidity and mortality during the COVID-19
47 pandemic, with an elevated risk for severe outcomes [1-3]. From the onset of the pandemic
48 in early 2020 to December 2022, there were 24,203 cases of COVID-19 among pregnant
49 women in the United States with 2,043 fatalities [4]. This 8.4% mortality rate is significantly
50 higher than that of the general population (0.061%), reflecting the elevated risk for disease
51 outcomes in pregnancy. Pregnant women also were more likely to require hospitalization
52 and invasive ventilation from acute SARS-CoV-2 infection than non-pregnant women [3, 4].
53 Adverse pregnancy and neonatal outcomes were an additional concern, as SARS-CoV-2
54 infection has been associated with preeclampsia, stillbirth, NICU admission, and preterm
55 birth in women [1, 5-9] and mouse models [10].

56 The Centers for Disease Control and Prevention [11] and the American College of
57 Obstetricians and Gynecologists (ACOG) recommend vaccination during pregnancy to
58 provide optimal protection against SARS-CoV-2 for both the mother and fetus [12]. Data
59 from November 2021 show vaccination rates among pregnant women (45.1%) were
60 significantly lower than that of non-pregnant people (64.9%) [13]. Vaccination rates among
61 pregnant women have since fallen precipitously, and remain lower than the general
62 population, with less than 15% of pregnant women vaccinated in the 2023-2024
63 vaccination season [14]. This decline in vaccine uptake is particularly concerning given that
64 other vaccines offered during pregnancy, such as influenza and Tdap, show higher coverage
65 rates (47.4% and 59.6%, respectively) [15, 16]. Despite a favorable benefit of administering

66 COVID-19 vaccines during pregnancy [17-19], low vaccine uptake may be a result of greater
67 vaccine hesitancy in this population [20-25].

68 While vaccination is the best preventative strategy to reduce the severity of COVID-
69 19 outcomes [17, 26], existing evidence suggests pregnant women mount dampened
70 immune responses to vaccination, highlighting the need for deeper immunological
71 assessments [27]. Previous studies of COVID-19 vaccines in pregnant women have
72 focused on placental antibody transfer following vaccination during pregnancy,
73 demonstrating the benefits of maternal vaccination in protecting newborns and infants
74 from severe infection [28-30]. While several studies have aimed to compare the antibody
75 landscape induced by vaccination during pregnancy with those in non-pregnant women
76 [31], to date, the effects of pregnancy on cross-protection against circulating variants in
77 addition to vaccine antigens have remained unexplored.

78 Using systems serology, we can broadly and deeply characterize the antibody
79 landscape in response to COVID-19 vaccination. By employing this systematic and
80 comprehensive approach, we can gain insight to shape future vaccine development and
81 public-health campaigns by understanding the protective immune response generated by
82 vaccination [32]. Combining functional assays and systems serology methods, we show
83 that the breadth and diversity of antibody generated by vaccination and polyfunctionality of
84 spike-specific memory CD4+ T cells are reduced during pregnancy.

85

86 **Methods**

87 ***Study Design***

88 Pregnant women were enrolled into mRNA vaccine studies at the Johns Hopkins Maternal
89 & Fetal Medicine Clinic (IRB 00246472) (n=7 pregnant) during the 2022-2023 vaccination
90 season. Pregnant women were contacted at clinical visits or via phone to determine
91 interest and eligibility. Women were eligible if they planned to receive an mRNA COVID
92 booster vaccine (Pfizer of Moderna) during weeks 32 through 36 of pregnancy, and consent
93 to maternal blood collection before and after receipt of the booster vaccine. Patients who
94 had already received an initial dose(s) of the vaccine were still eligible to enroll. Throughout
95 recruitment, 232 pregnant women were approached to participate in this study. Ninety-one
96 patients were initially interested while only 14 enrolled in the study. Of these, 7 completed
97 the study. For non-pregnant female comparators, samples were obtained from age-
98 matched adult female healthcare workers who were recruited during the 2022-2023
99 influenza vaccine enrollment period by fliers, emails, and announcements about the
100 annual vaccination program and were able to self-enroll upon receipt of the influenza
101 vaccine at the Johns Hopkins East Baltimore hospital (IRB00288258) (n = 13 non-pregnant).
102 Demographic information is detailed in **Table 1**. Of the vaccinees enrolled, 13 age-matched
103 non-pregnant females received the COVID-19 booster vaccine during the same vaccination
104 season and had pre- and post-vaccination blood samples available. Plasma and peripheral
105 blood mononuclear cells were obtained prior to and one month after receipt of mRNA
106 booster vaccines from pregnant and non-pregnant females. Plasma was used to assess
107 antigen-specific immunoglobulin isotype responses and live virus neutralizing antibody
108 responses, in addition to the crystallizable fragment (Fc) receptor affinity and non-

109 neutralizing antibody functions. Cryopreserved PBMCs were used for flow-cytometry
110 analyses.

111 ***Cells and Viruses***

112 VeroE6-TMPRSS2 cells were obtained from the cell repository of the National
113 Institute of Infectious Diseases, Japan, and were grown in complete medium consisting of
114 Dulbecco's modified Eagle's medium (DMEM) (Gibco, Thermo Fisher Scientific),
115 containing 10% fetal bovine serum (FBS) (Gibco, Thermo Fisher Scientific), 1 mM glutamine
116 (Invitrogen, Thermo Fisher Scientific), 1 mM sodium pyruvate (Invitrogen, Thermo Fisher
117 Scientific), 100 U/mL penicillin (Invitrogen, Thermo Fisher Scientific), and 100 µg/mL
118 streptomycin (Invitrogen, Thermo Fisher Scientific). Cells were incubated at 37°C in a
119 humidified incubator with 5% CO_2.

120 Ancestral (hCoV-19/USA/DC-HP00007/2020; B.1, GISAID EPI_ISL_434688), BA.5
121 (hCoV-19/USA/MD-HP32103-PIDCNSQVGY/2022, GISAID EPI_ISL_15013106), XBB.1.5
122 (hCoV-19/USA/MD-HP40900-PIDYSWHNUB/2022, GISAID EPI_ISL_16026423), and JN.1
123 (hCoV-19/USA/MD-HP49672-PIDDVSVURS/2023, GISAID EPI_ISL_18623285) variants of
124 SARS-CoV-2 were isolated in VeroE6-TMPRSS2 cells plated in 24-well plates as previously
125 described [33]. The consensus sequence of the virus isolate did not differ from the
126 sequence derived from the clinical specimen. The infectious virus titer was determined on
127 Vero-E6-TMPRSS2 cells using a 50% tissue culture infectious dose (TCID50) assay as
128 described [34].

129 ***Microneutralization assays***

130 Plasma neutralizing antibodies [35] were determined as described for SARS-CoV
131 and modified for SARS-CoV-2 as described [36]. Two-fold dilutions of plasma, starting at a
132 1:20 dilution, were made using incomplete medium (IM) - Dulbecco's modified Eagle's
133 medium (DMEM) (Gibco, Thermo Fisher Scientific), containing 1 mM glutamine (Invitrogen,
134 Thermo Fisher Scientific), 1 mM sodium pyruvate (Invitrogen, Thermo Fisher Scientific), 100
135 U/mL penicillin (Invitrogen, Thermo Fisher Scientific), and 100 µg/mL streptomycin
136 (Invitrogen, Thermo Fisher Scientific). Infectious virus was added to the plasma dilutions at
137 a final concentration of 1 × 10^3 TCID50/mL or 100 TCID50 per 100 µL. The plasma-virus
138 solution was incubated at room temperature for 1 hour, and 100 µL of each dilution was
139 added to 1 well of a 96-well plate of VeroE6-TMPRSS2 cells in hextuplicate. The cells were
140 incubated for 6 hours at 37°C with 5% CO_2. The inoculum was replaced with fresh IM, and
141 the cells were incubated at 37°C with 5% CO_2 for 3-4 days until cytopathic effect (CPE) is
142 evident in the no serum controls. The cells were fixed by the addition of 100 µL of 4%
143 formaldehyde for at least 4 hours at room temperature, and then stained with naphthol
144 blue-black overnight. The nAb titer was calculated as the highest serum dilution that
145 eliminated the CPE in 50% of the wells (NT50), and the AUC was calculated [37, 38].

146 ***Antigen-bead coupling***

147 Antigen-specific isotyping and Fc-receptor binding affinity were multiplexed using a
148 Luminex Intelliflex in a 384-well format. Antigens used in this panel are as follows:
149 ancestral spike (S) and nucleocapsid (N) protein, BA.5, XBB.1.5, and JN.1 spike proteins
150 were obtained through the National Cancer Institute Serological Sciences Networks
151 (SeroNet) for COVID-19 [39]. Each antigen was coupled to unique bead MagPlex bead

152 regions (Luminex). Briefly, beads were activated by activation solution consisting of
153 activation buffer (0.1M NaH2PO4; pH 6.2), 50mg/mL 1-ethyl-3-[3-dimethylaminopropyl]
154 carbodiimide (EDC), and 50mg/mL Sulfo-NHS (N-hydroxysulfosuccinimide). Activated
155 beads were coupled to 25ug of antigen in coupling buffer (0.05M MES; pH 5.0). Activated
156 coupled beads were blocked with blocking buffer (PBS 1X, 0.1% BSA, 0.02% Tween-20,
157 0.05% sodium azide; pH 7.4), washed with washing buffer (PBS 1X, 0.05% Tween-20) and
158 stored at 4°C in PBS.

159 ***Luminex serological assays***

160 Serum was diluted 1:25 and was incubated with bead solution (20 µL of each bead
161 region in 20 mL of Luminex Assay Buffer: PBS 1X, 0.1% BSA, 0.05% Tween-20). This
162 protocol was followed for isotyping (IgM, IgG [IgG1-4], and IgA [IgA1-2]) and binding to the
163 following Fc receptors (FcRs): FcγRIIA-R, FcγRIIA-H, FcγRIIb, FcγRIIIA-V, FcγRIIIA-F,
164 FcγRIIIB, FcRn, and FcαR (Duke Vaccine Institute – Protein Production facility). Following
165 incubation, plates were placed on a magnet and washed with Procartaplex Wash Buffer
166 (ThermoFisher). Each assay plate was then incubated with 45 µL of secondary antibody
167 diluted in Luminex Assay Buffer. Isotypes were identified by PE-conjugated antibodies
168 (Southern Biotech) and FcR proteins were biotinylated using BirA biotin-ligation kit (Avidity)
169 at least one day prior and coupled to PE-Streptavidin (BioLegend). Following incubation
170 with secondary antibody, plates were placed on a magnet and washed. Beads were
171 resuspended in Procartaplex Wash Buffer before running on the Luminex Intelliflex.
172 Samples were run on FlexMap 3D Low with a DD range of 7000-1700. For each assay, the
173 MFI of secondary antibody-conjugated to PE, or FcR protein-conjugated to PE for each

174 bead region was measured on the Luminex Intelliflex to quantify antigen-specific
175 immunoglobulin isotypes and FcR responses in each sample at 0- and 28-days post
176 vaccination [40].

177 ***Antibody-dependent complement deposition (ADCD)***

178 Serum (1:15 dilution) was added to the MagPlex antigen coated beads. Plates were
179 incubated, placed on a magnet, and washed 3 times with 1% BSA. Lyophilized Low-Tox
180 Guinea Pig Complement (Cedarlane) was reconstituted in ice-cold dH2O and diluted 1:25
181 in Gelatin Veronal buffer with Mg^{2+} & Ca^{2+} (GVB++) (Boston Bio). Diluted complement
182 protein was added to each well followed by incubation at 37C. IgG goat anti-guinea pig C3
183 (MP Biomedicals) was diluted 1:500 in 0.1% BSA and added to each well. After incubation,
184 Donkey-anti goat IgG secondary antibody-PE (ThermoFisher) was diluted 1:200 in 0.1% BSA
185 and added to each well. Beads were resuspended in 0.1% BSA and run on the Luminex
186 Intelliflex.

187 ***Antibody-dependent NK-cell cytotoxicity (ADNK)***

188 Natural killer (NK) cells were isolated from donor blood. Whole blood was
189 centrifuged through a Ficoll gradient to harvest PBMCs and NK cells isolated from PBMCs
190 using the MagniSort™ Human NK-cell Enrichment Kit (ThermoFisher) with adjustment to a
191 final concentration of 1.5 x 10^6 cells/mL in R10 medium, and IL-15 (1 ng/mL, Abcam) was
192 added and incubated overnight. Plates were coated with 3 mg/mL antigen (ancestral, BA.5,
193 XBB.1.5, and JN.1 spike proteins – SeroNet), blocked with 5% BSA, washed, and dried
194 before adding serum (1:100 dilution). Inhibitor cocktail (2.5 µL CD107a-PeCy5 (BD
195 Bioscience - BDB555802) + 0.5 mL BFA (Millipore Sigma) + 1 µL Golgi Stop (BD Bioscience)

196 + 9 mL R10 medium) was added to each well, incubated, and surface staining cocktail (1 µL
197 CD3-Pacific Blue (BD Bioscience - BDB558117) + 1mL CD56-PE-Cy7 (BD Bioscience -
198 BDB557747) + 1 mL CD16-APC-Cy7 (BD Bioscience - BDB557758) + 7 mL PBS) is added to
199 a V-bottom 96-well plate. NK cells were transferred to the V-bottom 96 well plate with pre-
200 added surface stain cocktail and incubated. Cells were pelleted, supernatant removed,
201 and Perm A (ThermoFisher) was added to each well. Cells were washed and Intracellular
202 staining cocktail (1 mL IFNγ-APC (BD Bioscience -) + 1 mL MIP1-B-PE (BD Bioscience -
203 BDB550078) + 48 mL Perm B (ThermoFisher) was added to each well. Plates were washed,
204 cells were resuspended in PBS and run on a Symphony A3 through the Bloomberg Flow
205 Cytometry and Immunology Core. Gating strategy as follows: NK cells- CD3-, CD16+,
206 CD56+ with reported cell populations including IFNγ+, CD107a+ and MIP-1β + NK cells.

207 ***Antibody-dependent neutrophil phagocytosis (ADNP)***

208 Antigens (ancestral, BA.5, XBB.1.5, and JN.1 spike proteins – SeroNet) were
209 biotinylated with the BirA biotin-ligation kit (Avidity) and coupled to FluoSpheres™
210 NeutrAvidin™-Labeled Microspheres, 1.0 µm, yellow-green fluorescent (505/515)
211 (ThermoFisher). Antigen was combined with Neutravidin beads and incubated. Serum was
212 diluted 1:100 in PBS and incubated with antigen coated beads. During incubation, cells
213 were isolated from donor blood. Whole blood was collected into CPT tubes and centrifuged
214 at 1000 rpm for 30 min. Granulocytes were collected from below the density gradient. Cells
215 were suspended 1:10 in ACK Lysis buffer and incubated at RT for 5 min to lyse red blood
216 cells. Cells were washed and resuspended in 10 mL of PBS. Plates were washed with PBS,
217 200 mL of neutrophil solution (5 x 10^6 cells/plate) was added to each well, incubated,

218 spun at 500g for 5 min, and cells were resuspended in extracellular staining solution (0.5
219 mL APC CD66b (BioLegend - 305117) + 19.5mL PBS / well) and incubated for 15min
220 covered with foil at RT. After staining, plates were washed and resuspended in 4% PFA to fix
221 cells, washed and resuspended in PBS. Plates were run on the Attune NxT flow cytometer.
222 Gating on CD66b+ cells (neutrophils) followed by bead+ neutrophils, stained with APC.
223 Data are reported as a PhagoScore, calculated as (% bead-positive neutrophils) *
224 (geometric MFI of each cell) [41].

225 ***Antibody-dependent cellular phagocytosis (ADCP)***

226 THP-1 cells, a human monocytic cell line, were plated 2.5 x 10^4 per well. Cells were
227 grown in suspension and diluted with warm R10 medium. Following immune complex
228 formation, assay plates are washed with PBS and centrifuged at 2000g for 10 min. The THP-
229 1 cells were added, and plates were incubated O/N at 37°C. THP-1 cells were fixed,
230 washed, and resuspended in PBS. Plates are run on the Attune NxT flow cytometer. Gating
231 included bead+ single-cells stained with APC, representing THP-1 cells that have
232 phagocytosed bead. Data are reported as a PhagoScore, calculated as (% bead-positive
233 neutrophils) * (geometric MFI of each cell) [42].

234 ***Ex vivo flow cytometry staining***

235 PBMCs were used to assess phenotype and function of immune cells. For broad
236 immune cell phenotyping (BIP), cells were stained for viability with Biolegend Live/Dead
237 Zombie NIR Fixable Viability Dye (423105) and BD Biosciences Fc Block™ (564219). Cell-
238 surface staining was performed with surface-antibody-cocktail mix (**Supplementary**
239 **Methods Table 1A**). Cells were fixed and permeabilized with a 1X Fixation/Permeabilization

240 buffer from eBioscience FoxP3/Transcription Factor Staining Buffer Set. Intracellular
241 staining was performed with intracellular antibody-cocktail mix (**Supplementary Methods**
242 **Table 1B**). Cells were resuspended in 1% paraformaldehyde and run on the 4-laser (16UV-
243 16V-15B-8R) Cytek Biosciences Aurora spectral flow cytometer. Data were exported for
244 further analysis in FlowJo for analysis (**Supplemental Figure 4**).

245 Intracellular cytokine-flow cytometry staining was used to assess antigen-specific
246 cytokine production and T-cell phenotypic and functional profiles. Cryopreserved PBMCs
247 were thawed, rested, and cultured overnight with 1 mg/mL peptide pools consisting of 315
248 peptides (15-mers with 11 amino acid overlap) spanning the ancestral SARS-CoV-2 spike
249 protein (JPT Peptide Technologies, PM-WCPV-S-1) or a DMSO (unstimulated) control. After
250 overnight incubation, cells were washed and stained for flow cytometry as described for
251 BIP with the following variation: staining for viability was with Invitrogen Live/Dead Fixable
252 Blue Dead Cell Stain (L34962) and with T-cell panel surface and intracellular cytokine-
253 antibody cocktails (**Supplementary Methods Table 2A-B**). For ICS, data were processed
254 using biexponential transformation and exported for further analysis in FlowJo to assess
255 cytokine-producing, antigen-specific T cells (**Supplemental Figure 5**). Polyfunctionality of
256 these T cells was analyzed with Pestle v2.0 and SPICE 6 v6.1.

257 ***Statistical analyses***

258 GraphPad Prism v10.1 was used to perform univariate analyses with details about
259 statistical tests used for each dataset in figure legends. Spearman correlations of systems
260 serology measures were visualized in heatmaps generated using R v4.2.3 and version
261 1.0.12 of the package "pheatmap" (https://cran.r-project.org/web/packages/pheatmap

262 [43]. For ADNP and ADNK assays, data were averaged across two healthy donors. Flow FCS
263 files were analyzed using FlowJo v10 (10.8.1) software. Gating strategy for BIP and ICS can
264 be found in **Supplementary Figures 1** and **2**, respectively. ICS and BIP data were exported
265 from Pestle v2.0 and SPICE 6 v6.1 for further statistical analyses detailed in figure legends.
266

267 **Results**

268 ***Pregnancy alters IgG subtype dominance in response to novel variants***

269 Because SARS-CoV-2 nucleocapsid (N) antibodies are not generated by mRNA
270 vaccines targeted to S protein, this can be used as a proxy for SARS-CoV-2 infection [44],
271 with recognized limitations [35]. There was no increase in either anti-N IgG **(Figure 1A)** or in
272 any subclass of IgG **(Supplemental Figure 1A)** in any participants, suggesting that no one
273 was infected with SARS-CoV-2 during their study enrollment window. However, all
274 participants had detectable anti-N IgG levels highlighting prior exposure to SARS-CoV-2 in
275 our cohort. Luminex-bead assays were used to comprehensively characterize the antibody
276 response generated by vaccination against SARS-CoV-2 vaccine antigens (ancestral and
277 BA.5 S) and other variants (XBB.1.5 and JN.1 S). COVID-19 boosters induced IgG in both
278 pregnant and non-pregnant females to vaccine and circulating variants **(Figure 1B)**. Prior to
279 vaccination, total IgG to ancestral S and BA.5 S was high in both cohorts, as SARS-CoV-2
280 exposure through infection and prior vaccination is pervasive in the general population
281 [45]. However, there were distinct differences in the IgG subtype dominating this response.
282 There was IgG1 subtype dominance among non-pregnant, but not pregnant, females
283 **(Figure 1C-F).** While IgG3 contributed to a small proportion of total IgG generated in

284 response to vaccination, pregnant women were more likely to induce anti-S IgG3 than non-
285 pregnant females **(Supplemental Figure 1 B-E).**

286 ***Pregnancy reduces the cross-neutralizing capacity of antibodies recognizing SARS-***
287 ***CoV-2 variants***

288 The ratio of IgG1:IgG3 has been shown to be predictive of SARS-CoV-2 neutralization
289 capacity [46]. Compared with non-pregnant females, pregnant women had reduced
290 IgG1:IgG3 ratios, particularly to circulating variants, (JN.1 $p = 0.02$, XBB.1.5 $p = 0.05$)
291 demonstrating that the dominant IgG1 response in non-pregnant females may be indicative
292 of broader cross-neutralization **(Figure 2A-D).** This was reflected by reduced live virus
293 neutralizing antibody titers in pregnant compared with non-pregnant women to variants
294 (JN.1 $p = 0.07$, XBB.1.5 $p = 0.03$). Both cohorts showed a rise ($p < 0.001$) in neutralizing-
295 antibody titers to ancestral and BA.5 viruses after vaccination and were able to effectively
296 neutralize these viruses **(Figure 2E-F)**. Pregnant women, however, had significantly lower
297 nAb titers than non-pregnant females, with many pregnant women failing to reach the limit
298 of detection **(Figure 2G-H)**. In response to XBB.1.5, while vaccination significantly
299 increased nAb titers in both groups, these responses were significantly higher in non-
300 pregnant than pregnant females. Likewise, among non-pregnant females, vaccination
301 boosted nAb titers against JN.1; there was, however, no vaccine-induced increase in nAb
302 titers among pregnant women, with only 2/7 surpassing the limit of detection. **(Figure 2G-**
303 **H)**. These data suggest that there is reduced breadth and cross-reactivity to variants after
304 COVID-19 boosting among pregnant compared with non-pregnant females.

305 ***Fc receptor affinity is not maintained in pregnant women against novel variants***

306 While neutralizing-antibody titers are considered a correlate of protection for SARS-
307 CoV-2 infection [47], non-neutralizing functions also are important and may contribute to
308 robust protection from severe disease [48]. Data from mouse models suggest FcR-binding
309 affinity and its associated effector functions are necessary for preventing severe COVID-19
310 disease [49]. To further understand protection provided by mRNA boosters in pregnant
311 women, we investigated FcR binding affinity. Antibody Fc binding affinity to FcγRIIA-R,
312 FcγRIIA-H, FcγRIIb, FcγRIIIA-V, FcγRIIIA-F, FcγRIIIB, FcRn, and FcαR was assessed by a
313 multiplexed Luminex bead assay. FcR-binding affinity was similarly induced by vaccination
314 in response to ancestral and BA.5 vaccine antigens among both non-pregnant and
315 pregnant females **(Figure 3A-B).** While non-pregnant females saw similar increases in FcR
316 affinity to non-vaccine antigens following vaccination, vaccination did not induce changes
317 in FcR affinity in pregnant women, with no increase in affinity to 4/6 FcγRs in response to
318 XBB1.5 and 2/6 FcγRs in response to JN.1 (**Figure 3C-D**).

319 ***Non-neutralizing antibody functions and nAb are negatively correlated among***
320 ***pregnant women***

321 In order to understand how Fc-binding affinity contributes to immunity generated by
322 COVID-19 vaccination, several non-neutralizing antibody functions were assessed. Non-
323 neutralizing functions aid in the clearance of infected cells through recruiting effector cells
324 [50]. Antibody-dependent complement deposition (ADCD) was analyzed with a
325 multiplexed Luminex bead assay to measure antibody binding to complement protein C3
326 as a broad indicator of the ability of serum antibody to induce activation of the
327 complement cascade [40]. ADCD was induced by vaccination in both cohorts in response

328 to only XBB.1.5. (**Figure 4A**). As ADCD to ancestral and BA.5 S was high in pre-vaccination
329 samples, it is likely that there were high preexisting immune responses through
330 complement activation in both cohorts.

331 In pregnancy, macrophage inflammatory protein (MIP)-1β+ NK cells are found at the
332 maternal-fetal interface and are important for successful implantation and placentation
333 [51]. In NK cells, MIP-1β acts as a chemoattractant in response to activation [52]. Antibody-
334 dependent NK-cell cytotoxicity (ADNK) can be measured through MIP-1β production by NK
335 cells [53]. MIP-1β+ NK cells were uniquely elevated in pregnant women following
336 vaccination when compared with non-pregnant females (**Figure 4B**). In NK cells, interferon
337 gamma (IFNγ) acts as an antiviral cytokine to promote further accumulation, activation,
338 and cytotoxicity of NK cells [54]. As an additional readout of ADNK, NK cell IFNγ production
339 post-vaccination was elevated in pregnant women in response to BA.5 S and in non-
340 pregnant females in response to JN.1 S **(Supplemental Figure 2A).** There were no changes
341 post-vaccination in NK-cell degranulation, as marked by CD107a+ NK cells, among either
342 cohort **(Supplemental Figure 2B)**.

343 Antibody-dependent cellular phagocytosis (ADCP) and antibody-dependent
344 neutrophil phagocytosis (ADNP) assess the ability of antibody to induce macrophage and
345 neutrophil phagocytosis of antigen, respectively, and are reported as a PhagoScore [41],
346 representing both the function and number of beads phagocytosed. ADCP and ADNP
347 decreased following vaccination against vaccine and variant antigens (**Figure 4C-D**). This is
348 likely indicative of a shift towards neutralization and away from non-neutralizing cellular
349 functions, a phenomenon that has been documented in the context of repeat vaccination

350 and may be a result of immune imprinting mechanisms [55]. Correlation analyses revealed
351 significant negative correlations between nAb titers and ADNP PhagoScores among
352 pregnant women only, further suggesting a shift away from neutralization, and towards
353 non-neutralizing neutrophil phagocytosis among pregnant women (**Figure 4E-H**). In non-
354 pregnant females, correlations were not significant, suggesting antibody responses marked
355 by both cellular non-neutralizing and neutralizing-antibody function, indicative of a more
356 comprehensive and multi-pronged immune response generated by vaccination.

357 ***Altered correlations among IgG subclasses and antibody functional phenotypes in***
358 ***pregnant women***

359 Correlation matrices can be used to examine complex relationships between
360 antibody isotypes and effector functions assessed by systems serology [56]. These
361 analyses can highlight isotype dependence and may reveal differences in subclass
362 functionality [56]. Spearman correlation matrices were generated to assess correlations
363 between Ig isotypes and FcR affinity and antibody functional properties post-vaccination in
364 response to vaccine and variant viruses (**Figure 5**). Matrices were most different between
365 pregnant and non-pregnant women for variants, with fewer strong correlations in pregnant
366 than non-pregnant women. Among non-pregnant women, IgG1 was positively and IgG3
367 was negatively correlated with FcR binding as well as neutralizing and non-neutralizing
368 antibody functions, particularly against variants. This trend was reversed in pregnant
369 women, with positive trends with IgG3 and negative trends with IgG1. These data further
370 implicate the reduced IgG1:IgG3 ratio and isotype subclass switching as functionally
371 altering antibody-mediated immunity in pregnant women.

372 ***Decreased polyfunctional CD4⁺ T cells responses in pregnant women***

373 Because immunoglobulin subtype switching depends on CD4⁺ T-cell help and
374 cytokine production [57], we hypothesized that differences in CD4⁺ T-cell cytokine
375 production between pregnant and nonpregnant females might contribute to differences in
376 isotype switching and IgG subtypes. We assessed intracellular-cytokine production by
377 CD4+ T cells in pregnant and non-pregnant women in response to ancestral S-peptide
378 pools [58, 59]. Intracellular cytokine staining of CD4+ T cells in response to ancestral S-
379 peptide stimulation at post-vaccination timepoints demonstrated IFNγ+ monofunctional
380 dominance in pregnant women, represented by an expansion of the dark purple slice
381 (**Figure 6A**). In CD4+ T cells, IFNγ production is known to modulate class switching in B
382 cells, particularly favoring IgG3 over IgG1 [60-62]. Conversely, non-pregnant female
383 participants demonstrated more broadly polyfunctional CD4+ T-cell responses, defined as
384 producing two or more cytokines and highlighted by the arcs (**Figure 6B**). A greater
385 proportion of polyfunctional CD4+ T cells in the non-pregnant females were IL-21+,
386 represented by the green arc (**Figure 6B**). IL-21 is a cytokine that induces B cells to
387 differentiate into antibody-secreting cells [63] and has been linked to improved antibody
388 responses to vaccination [58, 64-66]. Polyfunctional CD4+ T-cell responses can enhance
389 nAb titers and immunity following vaccination against multiple pathogens, including SARS-
390 CoV-2 [67-69].

391 ***Polymorphonuclear myeloid-derived suppressor cells are increased during pregnancy***

392 Polymorphonuclear myeloid-derived suppressor cells (PMN-MDSCs) have
393 previously been studied in the context of pregnancy, as they are required to maintain

394 maternal-fetal tolerance and are critical for fetal development [70, 71]. Their role, however,
395 has not been defined in the context of vaccination during pregnancy. There were no
396 detectable PMN-MDSCs in nonpregnant women, whereas the percentage in pregnant
397 women ranged from 0 to 1.5% of live PBMCs (**Supplemental Figure 3A**). The percentage of
398 low-density neutrophils also tended to be greater in pregnant women (**Supplemental**
399 **Figure 3B**), but small sample sizes preclude deeper analysis. The percentages of both
400 PMN-MDSCs and neutrophils were negatively correlated with CD4+ T cell cytokine
401 production in pregnant women (**Supplemental Figure 3C**).
402

403 **Discussion**

404 Through broad characterization of the antibody landscape following COVID-19
405 vaccination, pregnancy was associated with reduced cross-reactive ntibody responses,
406 reflected in decreased IgG1:IgG3 ratios, nAb titers, and FcR-binding affinity in pregnant
407 compared with non-pregnant women. Previous studies have assessed the antibody profile
408 generated by COVID-19 vaccination during pregnancy [28, 31, 72], with a focus on
409 transplacental antibody transfer and protection of babies and infants from severe disease.
410 One study showed limited cross-recognition in pregnant women to non-vaccine antigens
411 after the first doses of ancestral vaccines, with no comparisons with non-pregnant controls
412 [28]. Our data illustrate that pregnancy is associated with reduced isotype class switching
413 and lower nAb responses to variants as compared with non-pregnant controls. Continuing
414 efforts to assess antibody responses to updated vaccines remains critical to
415 understanding cross-protection to variants in circulation.

416 SARS-CoV-2 has continued to rapidly evolve and mutate into new variants to escape
417 adaptive-immune responses [73]. In 2022, Omicron variants became dominant in
418 circulation, largely due to an ability to evade nAb generated by ancestral vaccines and
419 natural infections [74]. New variants with the ability to evade nAb continue to emerge and
420 dominate, with XBB.1.5. appearing in October 2022 and peaking in January of 2023, after
421 the inclusion of BA.5 in bivalent booster vaccines was established [75]. By the time XBB.1.5
422 monovalent boosters were accessible, a new variant, JN.1 caused 60% of global cases [75,
423 76]. A potential limitation of annual vaccines is mismatches between dominate circulating
424 strains and updated booster vaccines because variants continue to emerge between
425 annual vaccines strain updates [11, 77, 78]. While mRNA technology has increased the
426 speed in which companies can adapt updated vaccines to emerging variants, development
427 of a new booster vaccine still takes several months [79]. Thus, government officials and
428 researchers must work collaboratively to select strains for booster vaccines that will elicit
429 the greatest breadth of immunity [79]. In our study, almost all women were vaccinated
430 against ancestral and BA.5 (bivalent boosters), while XBB.1.5. was the dominant variant in
431 circulation. Our data provide mechanistic evidence that pregnant women have limited
432 cross-protective antibodies.

433 With repeated exposure to antigen through natural infection and booster vaccines,
434 antibody responses to COVID-19 vaccines have evolved and correlates of protection have
435 changed. Total IgG and nAb titers are considered adequate correlates of protection against
436 COVID-19, similar to other acute respiratory infectious diseases [80]. Recent data have
437 suggested that to mount sufficient protection, antibodies against SARS-CoV-2 must

438 possess both neutralizing and non-neutralizing functions as correlates of protection [81].
439 As nAb titers wane and symptomatic cases rise, hospitalization rates among the general
440 population remain low [82]. This provides evidence that other antibody characteristics may
441 be important for protection from severe disease. Our data demonstrate that pregnant
442 women have reduced FcR binding and nAb responses combined with elevated ADNK and
443 ADNP, especially to non-vaccine antigens.

444 Our data suggest that reduced class switching and T-cell polyfunctionality may
445 contribute to limited cross-reactivity of antibodies during pregnancy. There is trend for
446 PMN-MDSCs in PBMCs to be more frequent among pregnant than non-pregnant, which
447 might contribute to suppressed CD4+ T cell cytokine production and proliferation [36].
448 CD4+ T cells are critical for generation of high affinity, class switched antibodies and
449 contribute to vaccine-induced protection against COVID-19 [83]. IL-21+ CD4+ T cells are
450 correlated with enhanced vaccine responses, including COVID-19 vaccine responses [65].
451 Pregnant women showed reduced expansion of IL-21+ CD4+ T cells, potentially
452 contributing to reduced Ig class switching and the generation of nAb responses in pregnant
453 women [58, 64-66]. Additionally, expansion of IFNγ+ monofunctional CD4+ T cells may
454 further contribute to reduced IgG1:IgG3 ratios among pregnant women, as these cells
455 promote IgG3 bias in B cells [60-62].

456 The small sample size is a limitation of this study and was associated with challenges
457 recruiting pregnant women. Previous studies have shown the impact of trimester on
458 immune responses generated by COVID-19 vaccination [17, 84]. In the present study,
459 sample size limited our ability to assess trimester differences, with 6/7 pregnant females

enrolled in our study being vaccinated in the second trimester of pregnancy. While 232 pregnant women were approached during the study enrollment window, only 7 completed the study. This likely reflects the limited COVID-19 vaccine uptake among pregnant women, which we show is caused by numerous factors across the care continuum that contribute to COVID-19 vaccine hesitancy in this population. Identification of points of public-health intervention to effectively increase vaccine uptake among pregnant women is needed.

Acknowledgements. We thank the clinical coordinators and vaccinees for making this study possible. We are especially grateful to Kimberly Jones-Beatty and Michelle Ufua for their assistance with recruitment. Thank you to Galit Alter, Ryan McNamara, and Taras Chicz for graciously training lab members and sharing protocols to develop systems serology methods. We thank Prakash Srinivasan for the use of the Attune Nxt flow cytometer.

Funding. This study was supported by the Food and Drug Administration (FDA) of the U.S. Department of Health and Human Services (HHS) as part of a financial assistance award [Center of Excellence in Regulatory Science and Innovation grant to Johns Hopkins University, U01FD005946] totaling $415,256 with 75% percentage funded by FDA/ OWH. The contents are those of the author(s) and do not necessarily represent the official views of, nor an endorsement, by FDA/OWH, or the U.S. Government. FDA CERSI U01FD005942 (SLK), NIH NIAID 75N93021C00045 (AP, RR), NIH NCI U54 CA260492 (SLK, ALC).

482 **Data Availability**

483 All anonymized data that support the findings of this study can be made available upon
484 reasonable request.

485

486 **Author Contributions**

487 SLK, IB, AP, and ALC conceptualized the experimental design and group comparisons for
488 this study. MAP, H-SP, JSL, LStC, PS, IB, JS, KF, RR, and ALC identified, acquired, stored, and
489 distributed patient samples and clinical and demographic data for analyses. MAP, H-SP,
490 PC, AW and JSL developed and validated serological assays. MAP, JS, LG and H-SP
491 processed samples and completed technical assays. MAP, KR, and AY conducted
492 statistical analyses. MAP, LG, KR, ALC, and SLK developed all tables and figures. MAP, ALC,
493 SLK wrote the initial draft of the manuscript. All authors provided substantive edits and
494 approved the final draft of the manuscript.

495

496 **References**

497

498 1. Engjom, H.M., et al., *Perinatal outcomes after admission with COVID-19 in*
499 *pregnancy: a UK national cohort study.* Nature Communications, 2024. **15**(1): p.
500 3234.
501 2. Brioschi Dos Santos, A.P., et al., *The impact of COVID-19 on maternal death and*
502 *fetal death, a cohort study in Brazil.* PLoS One, 2023. **18**(8): p. e0290343.
503 3. St Clair, L.A., et al., *Reduced control of SARS-CoV-2 infection associates with lower*
504 *mucosal antibody responses in pregnancy.* mSphere, 2024. **9**(3): p. e0081223.
505 4. Strid, P., et al., *Coronavirus Disease 2019 (COVID-19) Severity Among Women of*
506 *Reproductive Age With Symptomatic Laboratory-Confirmed Severe Acute*
507 *Respiratory Syndrome Coronavirus 2 (SARS-CoV-2) Infection by Pregnancy Status-*
508 *United States, 1 January 2020-25 December 2021*. Clin Infect Dis, 2022. **75**(Suppl 2):
509 p. S317-s325.
510 5. Wei, S.Q., et al., *The impact of COVID-19 on pregnancy outcomes: a systematic*
511 *review and meta-analysis.* Cmaj, 2021. **193**(16): p. E540-e548.

6. Sessa, R., et al., *SARS-CoV-2 Infection in Pregnancy: Clues and Proof of Adverse Outcomes*. Int J Environ Res Public Health, 2023. **20**(3).
7. Garcia-Flores, V., et al., *Maternal-fetal immune responses in pregnant women infected with SARS-CoV-2*. Nat Commun, 2022. **13**(1): p. 320.
8. Verma, S., E.B. Carter, and I.U. Mysorekar, *SARS-CoV2 and pregnancy: An invisible enemy?* Am J Reprod Immunol, 2020. **84**(5): p. e13308.
9. Doss, J.D., et al., *A prospective cohort study of pregnancy outcomes following antepartum infection with SARS-CoV-2*. Pregnancy Hypertens, 2024. **37**: p. 101152.
10. Creisher, P.S., et al., *Adverse outcomes in SARS-CoV-2-infected pregnant mice are gestational age-dependent and resolve with antiviral treatment*. J Clin Invest, 2023. **133**(20).
11. CDC. *Staying Up to Date with COVID-19 Vaccines*. 2025 January 7, 2025 [cited 2025 March 25]; Available from: https://www.cdc.gov/covid/vaccines/stay-up-to-date.html.
12. Ciapponi, A., et al., *Safety of COVID-19 vaccines during pregnancy: A systematic review and meta-analysis*. Vaccine, 2023. **41**(25): p. 3688-3700.
13. Razzaghi, H., et al., *COVID-19 vaccination coverage and intent among women aged 18-49 years by pregnancy status, United States, April-November 2021*. Vaccine, 2022. **40**(32): p. 4554-4563.
14. CDC. *COVID-19 Vaccination Coverage, Pregnant Women, United States*. 2025 March 19 [cited 2025; Available from: https://www.cdc.gov/covidvaxview/weekly-dashboard/pregnant-persons-vaccination.html.
15. Razzaghi H, K.K., Calhoun K, et al., *Influenza, Tdap, and COVID-19 Vaccination Coverage and Hesitancy Among Pregnant Women — United States, April 2023*. MMWR Morb Mortal Wkly Rep, 2023.
16. Katherine E. Kahn, E.G., Hilda Razzaghi, Tara C. Jatlaoui, Tami H. Skoff, Sascha R. Ellington, Carla L. Black, *Flu, Tdap, and COVID-19 Vaccination Coverage Among Pregnant Women – United States, April 2024*. 2024.
17. Norman, M., et al., *Neonatal Outcomes After COVID-19 Vaccination in Pregnancy*. Jama, 2024. **331**(5): p. 396-407.
18. CDC. *COVID-19 Vaccination for Women Who Are Pregnant or Breastfeeding*. 2024 September 10, 2024; Available from: https://www.cdc.gov/covid/vaccines/pregnant-or-breastfeeding.html#:~:text=COVID%2D19%20vaccination%20during%20pregnancy,19%20before%20or%20during%20pregnancy.
19. Kumar, D., S. Verma, and I.U. Mysorekar, *COVID-19 and pregnancy: clinical outcomes; mechanisms, and vaccine efficacy*. Transl Res, 2023. **251**: p. 84-95.
20. Casubhoy, I., et al., *A scoping review of global COVID-19 vaccine hesitancy among pregnant persons*. npj Vaccines, 2024. **9**(1): p. 131.
21. Oliver, J., et al., *Drivers of COVID-19 vaccine hesitancy among women of childbearing age in Victoria, Australia: A descriptive qualitative study*. Vaccine: X, 2022. **12**: p. 100240.
22. Hsu, A.L., et al., *Sources of Vaccine Hesitancy: Pregnancy, Infertility, Minority Concerns, and General Skepticism*. Open Forum Infectious Diseases, 2021. **9**(3).

23. Shephard HM, M.S., Nestoridi E, et al. *Inequities in COVID-19 Vaccination Coverage Among Pregnant Persons*. MMWR Morb Mortal Wkly Rep 2023 September 29, 2023.
24. Anderson, M.R., E.J. Hardy, and C.L. Battle, *COVID-19 Vaccine Hesitancy during the Perinatal Period: Understanding Psychological and Cultural Factors to Improve Care and Address Racial/Ethnic Health Inequities*. Womens Health Issues, 2022. **32**(4): p. 317-321.
25. Ramonfaur, D., et al., *Determinants of COVID-19 vaccine hesitancy among pregnant persons*. J Am Pharm Assoc (2003), 2023. **63**(4): p. 1191-1196.
26. Chavan, M., et al., *COVID-19 Vaccination in Pregnancy: The Benefits Outweigh the Risks*. J Obstet Gynaecol Can, 2021. **43**(7): p. 814-816.
27. Kay, A.W. and C.A. Blish, *Immunogenicity and Clinical Efficacy of Influenza Vaccination in Pregnancy*. Front Immunol, 2015. **6**: p. 289.
28. Lopez, P.A., et al., *Placental transfer dynamics and durability of maternal COVID-19 vaccine-induced antibodies in infants*. iScience, 2024. **27**(3): p. 109273.
29. Munoz, F.M., et al., *COVID-19 booster vaccination during pregnancy enhances maternal binding and neutralizing antibody responses and transplacental antibody transfer to the newborn*. Vaccine, 2023. **41**(36): p. 5296-5303.
30. Cassidy, A.G., et al., *Assessment of Adverse Reactions, Antibody Patterns, and 12-month Outcomes in the Mother-Infant Dyad After COVID-19 mRNA Vaccination in Pregnancy*. JAMA Netw Open, 2023. **6**(7): p. e2323405.
31. Atyeo, C., et al., *COVID-19 mRNA vaccines drive differential antibody Fc-functional profiles in pregnant, lactating, and nonpregnant women*. Sci Transl Med, 2021. **13**(617): p. eabi8631.
32. Ackerman, M.E., D.H. Barouch, and G. Alter, *Systems serology for evaluation of HIV vaccine trials*. Immunol Rev, 2017. **275**(1): p. 262-270.
33. Fall, A., et al., *The displacement of the SARS-CoV-2 variant Delta with Omicron: An investigation of hospital admissions and upper respiratory viral loads*. EBioMedicine, 2022. **79**: p. 104008.
34. Dhakal, S., et al., *Sex Differences in Lung Imaging and SARS-CoV-2 Antibody Responses in a COVID-19 Golden Syrian Hamster Model*. mBio, 2021. **12**(4): p. e0097421.
35. Dhakal, S., et al., *Reconsideration of Antinucleocapsid IgG Antibody as a Marker of SARS-CoV-2 Infection Postvaccination for Mild COVID-19 Patients*. Open Forum Infect Dis, 2023. **10**(1): p. ofac677.
36. Lee, J.M., et al., *Three doses of COVID-19 mRNA vaccine induce class-switched antibody responses in inflammatory arthritis patients on immunomodulatory therapies*. Front Immunol, 2023. **14**: p. 1266370.
37. Li, M., et al., *Convalescent plasma with a high level of virus-specific antibody effectively neutralizes SARS-CoV-2 variants of concern*. Blood Adv, 2022. **6**(12): p. 3678-3683.
38. Klein, S.L., et al., *Sex, age, and hospitalization drive antibody responses in a COVID-19 convalescent plasma donor population*. J Clin Invest, 2020. **130**(11): p. 6141-6150.

39. Karger, A.B., et al., *The Serological Sciences Network (SeroNet) for COVID-19: Depth and Breadth of Serology Assays and Plans for Assay Harmonization*. mSphere, 2022. **7**(4): p. e0019322.
40. Chung, A.W., et al., *Dissecting Polyclonal Vaccine-Induced Humoral Immunity against HIV Using Systems Serology*. Cell, 2015. **163**(4): p. 988-98.
41. Karsten, C.B., et al., *A versatile high-throughput assay to characterize antibody-mediated neutrophil phagocytosis*. J Immunol Methods, 2019. **471**: p. 46-56.
42. Loos, C., et al., *Systems serology-based comparison of antibody effector functions induced by adjuvanted vaccines to guide vaccine design*. npj Vaccines, 2023. **8**(1): p. 34.
43. Kolde, R., *Pretty Heatmaps*. 2018. p. Implementation of heatmaps that offers more control over dimensions and appearance.
44. Gaeta, A., et al., *Anti-N SARS-CoV-2 assays for evaluation of natural viral infection*. J Immunol Methods, 2023. **518**: p. 113486.
45. Swadźba, J., et al., *High Concentration of Anti-SARS-CoV-2 Antibodies 2 Years after COVID-19 Vaccination Stems Not Only from Boosters but Also from Widespread, Often Unrecognized, Contact with the Virus*. Vaccines (Basel), 2024. **12**(5).
46. Chen, W., et al., *The kinetics of IgG subclasses and contributions to neutralizing activity against SARS-CoV-2 wild-type strain and variants in healthy adults immunized with inactivated vaccine*. Immunology, 2022. **167**(2): p. 221-232.
47. Sun, K., et al., *SARS-CoV-2 correlates of protection from infection against variants of concern*. Nature Medicine, 2024. **30**(10): p. 2805-2812.
48. Izadi, A. and P. Nordenfelt, *Protective non-neutralizing SARS-CoV-2 monoclonal antibodies*. Trends Immunol, 2024. **45**(8): p. 609-624.
49. Mackin, S.R., et al., *Fc-γR-dependent antibody effector functions are required for vaccine-mediated protection against antigen-shifted variants of SARS-CoV-2*. Nat Microbiol, 2023. **8**(4): p. 569-580.
50. Chandler, T.L., et al., *Protective mechanisms of nonneutralizing antiviral antibodies*. PLoS Pathog, 2023. **19**(10): p. e1011670.
51. Du, M.R., S.C. Wang, and D.J. Li, *The integrative roles of chemokines at the maternal-fetal interface in early pregnancy*. Cell Mol Immunol, 2014. **11**(5): p. 438-48.
52. Bluman, E.M., et al., *Human natural killer cells produce abundant macrophage inflammatory protein-1 alpha in response to monocyte-derived cytokines*. J Clin Invest, 1996. **97**(12): p. 2722-7.
53. Boudreau, C.M., et al., *Antibody-mediated NK cell activation as a correlate of immunity against influenza infection*. Nature Communications, 2023. **14**(1): p. 5170.
54. Lin, Q., et al., *IFN-γ-dependent NK cell activation is essential to metastasis suppression by engineered Salmonella*. Nature Communications, 2021. **12**(1): p. 2537.
55. Tortorici, M.A., et al., *Persistent immune imprinting occurs after vaccination with the COVID-19 XBB.1.5 mRNA booster in humans*. Immunity, 2024. **57**(4): p. 904-911.e4.
56. Atyeo, C., et al., *Distinct Early Serological Signatures Track with SARS-CoV-2 Survival*. Immunity, 2020. **53**(3): p. 524-532.e4.

57. Sha, Z. and R.W. Compans, *Induction of CD4(+) T-cell-independent immunoglobulin responses by inactivated influenza virus*. J Virol, 2000. **74**(11): p. 4999-5005.
58. Thompson, E.A., et al., *Heterologous versus homologous boosting elicits qualitatively distinct, BA.5-cross-reactive T cells in transplant recipients*. JCI Insight, 2023. **8**(10).
59. Roznik, K., et al., *COVID-19 vaccination induces distinct T-cell responses in pediatric solid organ transplant recipients and immunocompetent children*. NPJ Vaccines, 2024. **9**(1): p. 73.
60. Peng, S.L., S.J. Szabo, and L.H. Glimcher, *T-bet regulates IgG class switching and pathogenic autoantibody production*. Proc Natl Acad Sci U S A, 2002. **99**(8): p. 5545-50.
61. Alspach, E., D.M. Lussier, and R.D. Schreiber, *Interferon γ and Its Important Roles in Promoting and Inhibiting Spontaneous and Therapeutic Cancer Immunity*. Cold Spring Harb Perspect Biol, 2019. **11**(3).
62. Mohr, E., et al., *IFN-{gamma} produced by CD8 T cells induces T-bet-dependent and -independent class switching in B cells in responses to alum-precipitated protein vaccine*. Proc Natl Acad Sci U S A, 2010. **107**(40): p. 17292-7.
63. Wang, S., et al., *IL-21 drives expansion and plasma cell differentiation of autoreactive CD11chiT-bet+ B cells in SLE*. Nature Communications, 2018. **9**(1): p. 1758.
64. Pallikkuth, S., et al., *Upregulation of IL-21 receptor on B cells and IL-21 secretion distinguishes novel 2009 H1N1 vaccine responders from nonresponders among HIV-infected persons on combination antiretroviral therapy*. J Immunol, 2011. **186**(11): p. 6173-81.
65. Malahe, S.R.K., et al., *The role of interleukin-21 in COVID-19 vaccine-induced B cell-mediated immune responses in patients with kidney disease and kidney transplant recipients*. Am J Transplant, 2023. **23**(9): p. 1411-1424.
66. Fan, W., Y. Wan, and Q. Li, *Interleukin-21 enhances the antibody avidity elicited by DNA prime and MVA boost vaccine*. Cytokine, 2020. **125**: p. 154814.
67. Darrah, P.A., et al., *Multifunctional TH1 cells define a correlate of vaccine-mediated protection against Leishmania major*. Nat Med, 2007. **13**(7): p. 843-50.
68. Rakshit, S., et al., *Polyfunctional CD4 T-cells correlating with neutralising antibody is a hallmark of COVISHIELDTM and COVAXIN® induced immunity in COVID-19 exposed Indians*. npj Vaccines, 2023. **8**(1): p. 134.
69. Li, L., et al., *In-depth analysis of SARS-CoV-2-specific T cells reveals diverse differentiation hierarchies in vaccinated individuals*. JCI Insight, 2022. **7**(7).
70. Shi, M., et al., *Continuous activation of polymorphonuclear myeloid-derived suppressor cells during pregnancy is critical for fetal development*. Cellular & Molecular Immunology, 2021. **18**(7): p. 1692-1707.
71. Li, C., et al., *Upregulated TRAIL and Reduced DcR2 Mediate Apoptosis of Decidual PMN-MDSC in Unexplained Recurrent Pregnancy Loss*. Frontiers in Immunology, 2020. **11**.

72. Atyeo, C.G., et al., *Maternal immune response and placental antibody transfer after COVID-19 vaccination across trimester and platforms*. Nature Communications, 2022. **13**(1): p. 3571.
73. Markov, P.V., et al., *The evolution of SARS-CoV-2*. Nature Reviews Microbiology, 2023. **21**(6): p. 361-379.
74. Chi, W.Y., et al., *COVID-19 vaccine update: vaccine effectiveness, SARS-CoV-2 variants, boosters, adverse effects, and immune correlates of protection*. J Biomed Sci, 2022. **29**(1): p. 82.
75. Huiberts, A.J., et al., *Effectiveness of Omicron XBB.1.5 vaccine against infection with SARS-CoV-2 Omicron XBB and JN.1 variants, prospective cohort study, the Netherlands, October 2023 to January 2024*. Euro Surveill, 2024. **29**(10).
76. Rubin, R., *As COVID-19 Cases Surge, Here's What to Know About JN.1, the Latest SARS-CoV-2 "Variant of Interest"*. Jama, 2024. **331**(5): p. 382-383.
77. Han, X. and Q. Ye, *The variants of SARS-CoV-2 and the challenges of vaccines*. J Med Virol, 2022. **94**(4): p. 1366-1372.
78. Cobey, S., et al., *Concerns about SARS-CoV-2 evolution should not hold back efforts to expand vaccination*. Nat Rev Immunol, 2021. **21**(5): p. 330-335.
79. Monto, A.S., A.S. Lauring, and E.T. Martin, *SARS-CoV-2 Vaccine Strain Selection: Guidance From Influenza*. J Infect Dis, 2022. **227**(1): p. 4-8.
80. Regev-Yochay, G., et al., *Correlates of protection against COVID-19 infection and intensity of symptomatic disease in vaccinated individuals exposed to SARS-CoV-2 in households in Israel (ICoFS): a prospective cohort study*. The Lancet Microbe, 2023. **4**(5): p. e309-e318.
81. Goldblatt, D., et al., *Correlates of protection against SARS-CoV-2 infection and COVID-19 disease*. Immunol Rev, 2022. **310**(1): p. 6-26.
82. Mahrokhian, S.H., et al., *COVID-19 vaccines: Immune correlates and clinical outcomes*. Hum Vaccin Immunother, 2024. **20**(1): p. 2324549.
83. Kent, S.J., et al., *Disentangling the relative importance of T cell responses in COVID-19: leading actors or supporting cast?* Nature Reviews Immunology, 2022. **22**(6): p. 387-397.
84. Yang, Y.J., et al., *Association of Gestational Age at Coronavirus Disease 2019 (COVID-19) Vaccination, History of Severe Acute Respiratory Syndrome Coronavirus 2 (SARS-CoV-2) Infection, and a Vaccine Booster Dose With Maternal and Umbilical Cord Antibody Levels at Delivery*. Obstetrics & Gynecology, 2022. **139**(3): p. 373-380.

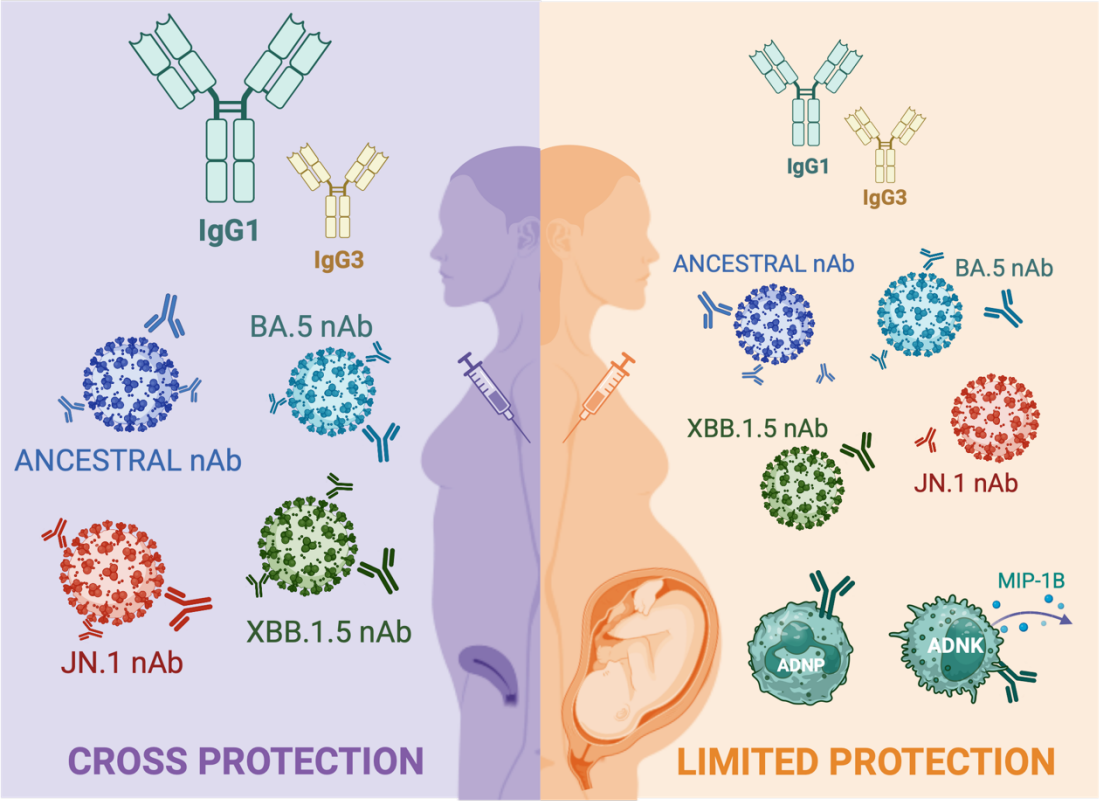

Graphical abstract

Table 1: Study Demographics

	Non-Pregnant n = 13	Pregnant n = 7	P-Value
Demographics	Mean ± SD	Mean ± SD	
Age	33.1 ± 6.1	32.9 ±3.2	0.93064
Vaccine Type			
Monovalent Booster	0 0%	2 28.5%	
Bivalent Booster	10 100%	5 71.5%	
Average Gestational Age (weeks)	-	22.4 ± 11.78	
	N %	**N %**	
Race			
White	8 61.5%	7 100%	
Black	2 15.4%	0 0%	
Asian	3 23.1%	0 0%	
Gestational Age (At Vaccination)	-	1st Trimester (n = 0) 0% 2nd Trimester (n = 6) 85.8% 3rd Trimester (n = 1) 14.2%	

Table 1.

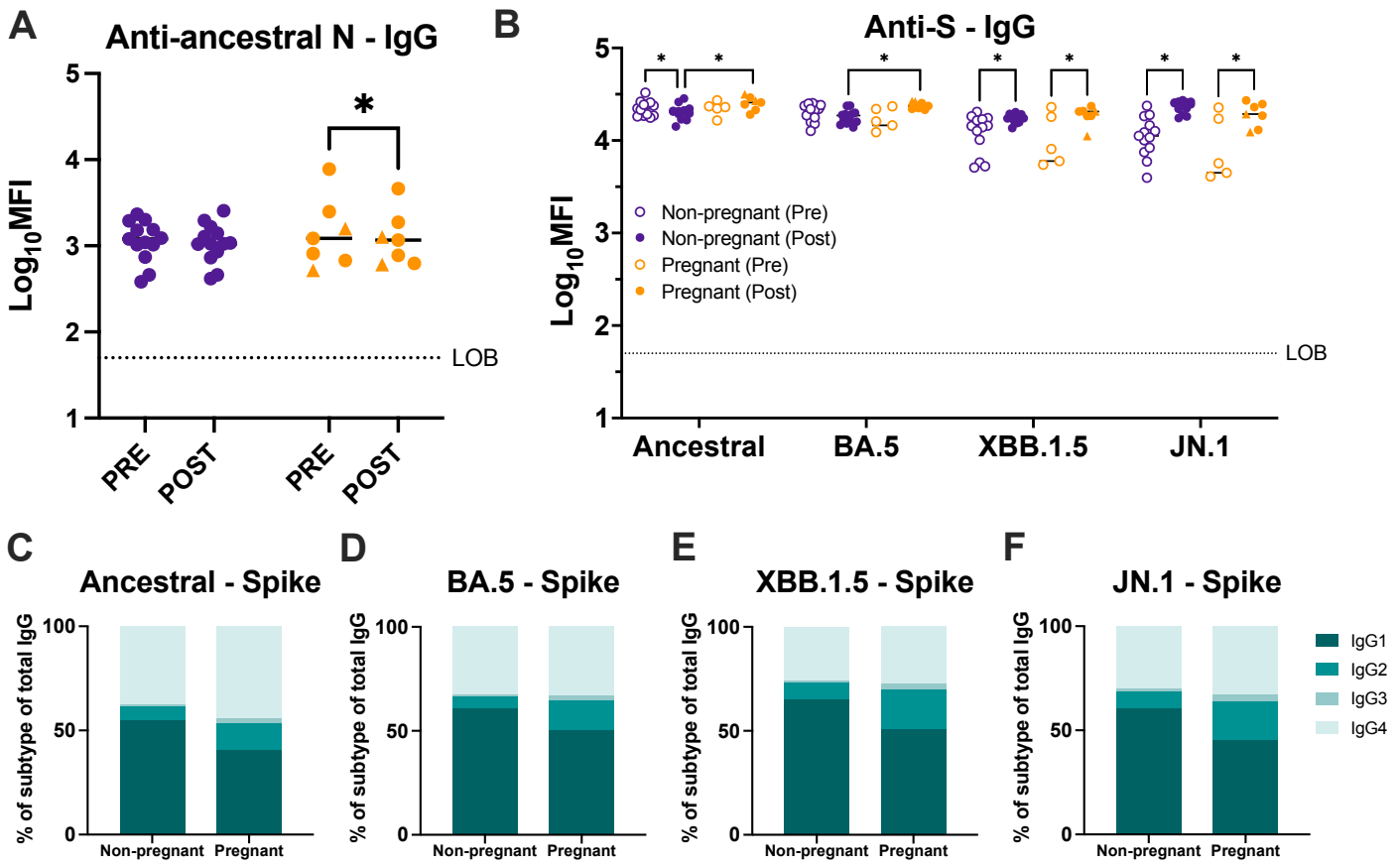

Figure 1. Vaccination differently induces IgG subtype responses during pregnancy. IgG antibody responses in serum pre and 3-5 weeks post-vaccination were measured by systems serology and reported as $\log_{10}$ mean fluorescence intensity (MFI). Pregnant individuals (n=7) are shown in orange and non-pregnant females (n=13) in purple. Triangles highlight individuals who received monovalent boosters and circles represent bivalent booster recipients. **(A)** Total IgG to ancestral nucleocapsid (N) protein**. (B)** Total IgG separated by SARS-CoV-2 vaccine (ancestral and BA.5) and variant (XBB1.5 and JN.1) spike (S) antigen and pregnancy status. **(C-F)** Relative abundance of IgG subtypes in pregnant and non-pregnant people as stacked bar plots representing each isotype as a percentage of Total IgG by **(C)** ancestral S, **(D)** BA.5 S, **(E)** XBB.1.5 S, and **(F)** JN.1 S. Data were analyzed by **(A)** repeated measures two-way ANOVA **(B-F)** linear mixed effects regression analysis with Bonferroni post-hoc. Asterisks indicate $p < 0.05$. Stippled line indicates limit of background (LOB) defined as the $\log_{10}$MFI of a defined negative control.

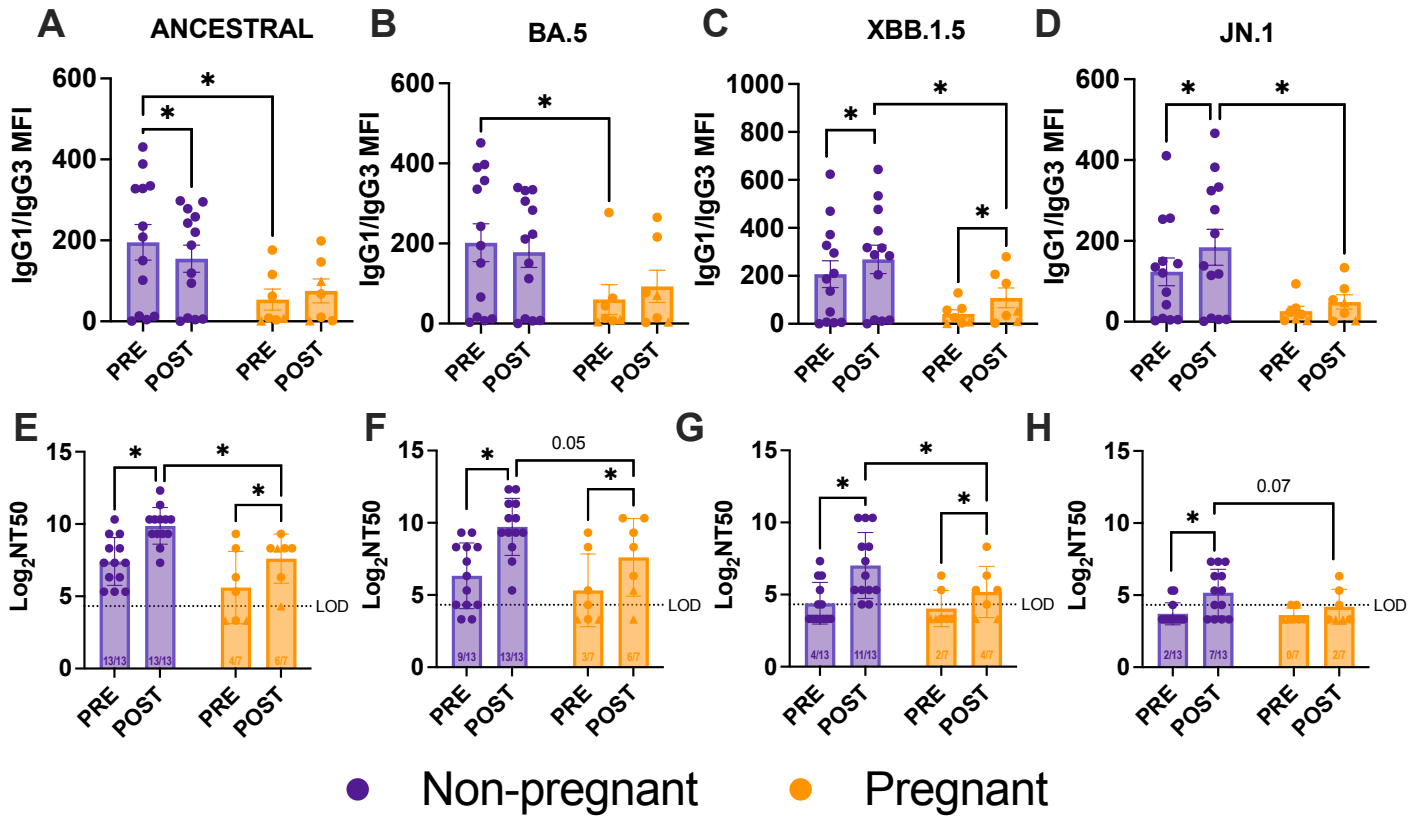

Figure 2. Pregnancy alters cross-neutralization of variants of concern. IgG antibody responses in serum pre and 3-5 weeks post-vaccination were measured by systems serology and reported as mean fluorescence intensity (MFI). Pregnant individuals (n=7) are shown in orange and non-pregnant females (n=13) in purple. Triangles highlight individuals who received monovalent boosters and circles represent bivalent booster recipients. **(A-E)** Ratio of IgG1:IgG3 antibodies specific to **(A)** ancestral spike (S), **(B)** BA.5 S, **(C)** XBB.1.5 S, and **(D)** JN.1 S. Neutralizing antibody (nAb) titers reported as Log_2 NT50 against live **(E)** ancestral, **(F)** BA.5, **(G)** XBB.1.5, and **(H)** JN.1 viruses. Ratios indicate number of individuals above the limit of detection (LOD) indicated by the stippled line. Data were analyzed by repeated measures two-way ANOVA with Bonferroni post-hoc. Asterisks indicate $p < 0.05$.

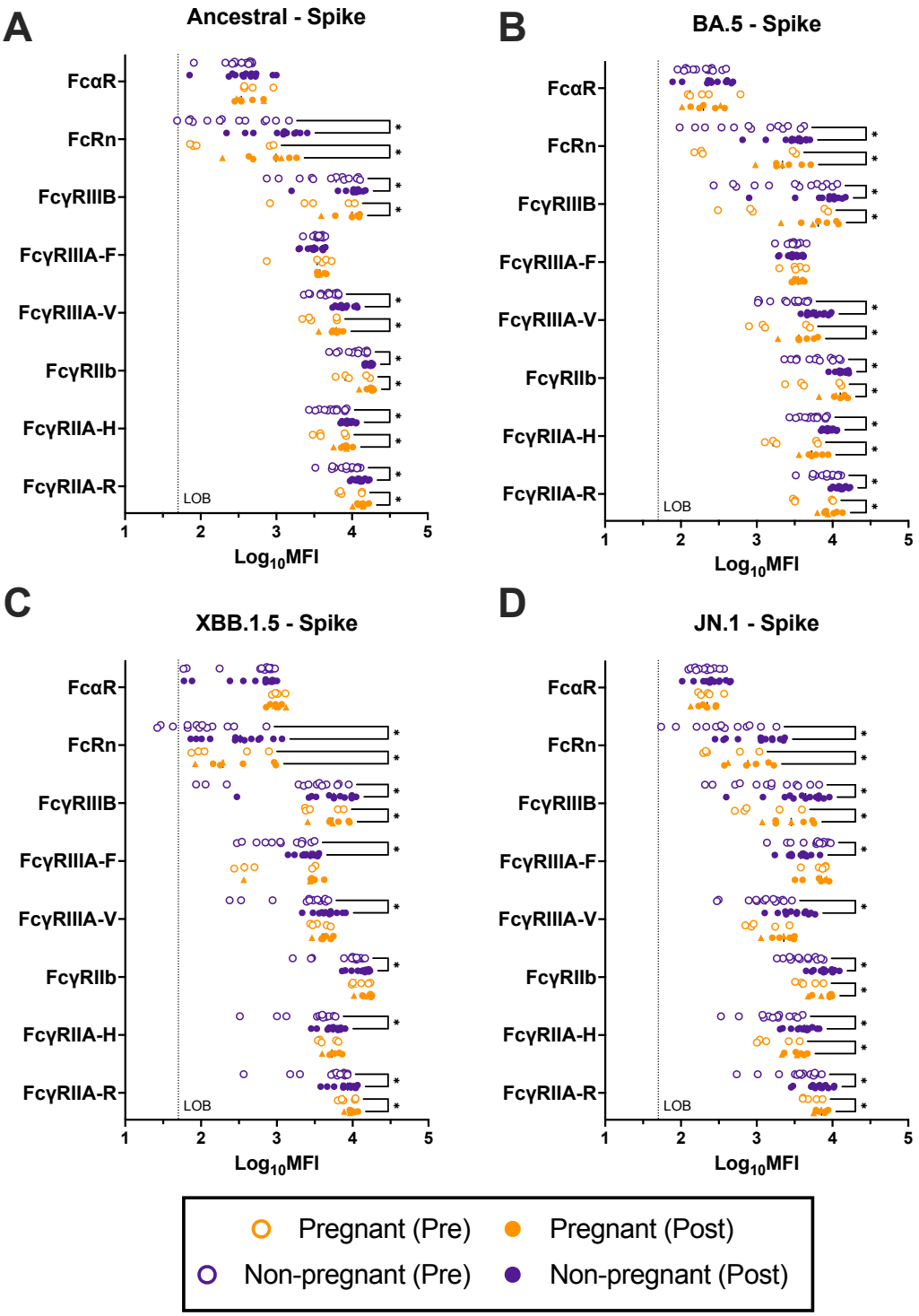

Figure 3. Fc receptor binding affinity is reduced in pregnant people in response to variants of concern. Serum antibody Fc receptor (FcR) binding affinity pre and 3-5 weeks post-vaccination were measured by multiplex Luminex bead assays and reported as $\log_{10}$ mean fluorescence intensity (MFI). Pregnant individuals (n=7) are shown in orange and non-pregnant females (n=13) in purple. Triangles highlight individuals who received monovalent boosters and circles represent bivalent booster recipients. Affinity for FcγRIIA-R, FcγRIIA-H, FcγRIIb, FcγRIIIA-V, FcγRIIIA-F, FcγRIIIB, FcRn, and FcαR was determined for **(A)** ancestral spike (S), **(B)** BA.5 S, **(C)** XBB.1.5 S, and **(D)** JN.1 S. Data were analyzed by linear mixed effects regression analysis with Bonferroni post-hoc. Asterisks indicate $p < 0.05$. Stippled line indicates limit of background (LOB) defined as the $\log_{10}$MFI of a defined negative control.

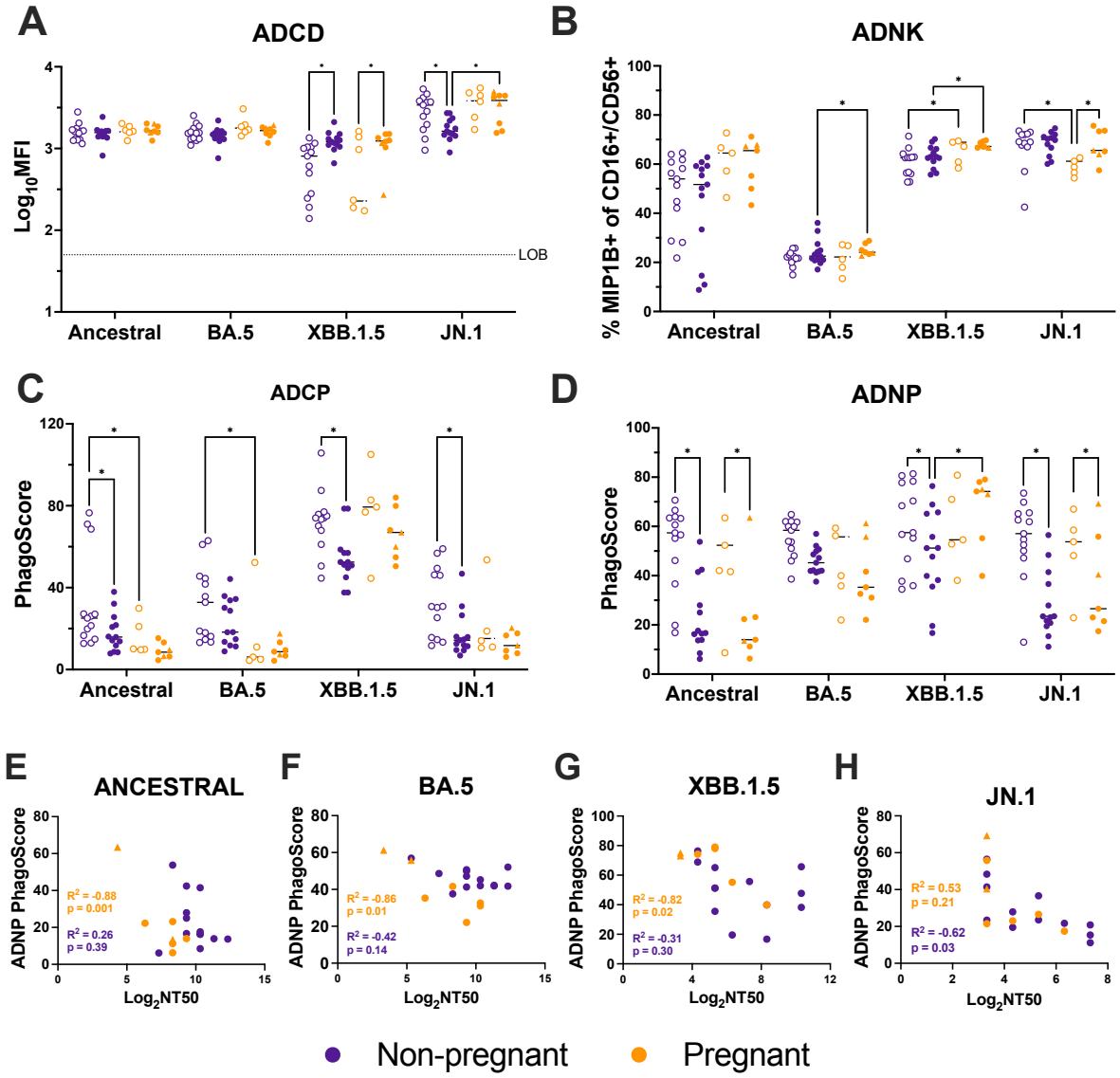

Figure 4. Non-neutralizing and neutralizing antibody functions are negatively correlated among pregnant individuals. Non-neutralizing antibody functions were measured pre and 3-5 weeks post-vaccination. Pregnant individuals (n=7) are shown in orange and non-pregnant females (n=13) in purple. Triangles highlight individuals who received monovalent boosters and circles represent bivalent booster recipients. **(A)** antibody dependent complement deposition (ADCD) was measured by assessing antibody affinity for C3 protein and is reported as $\log_{10}$ mean fluorescence intensity (MFI). Stippled line indicates limit of background (LOB) defined as the $\log_{10}$MFI of a defined negative control. NK cells isolated from donor blood were utilized to assess **(B)** antibody dependent NK cell cytotoxicity (ADNK), or the ability of antigen specific serum antibody to include NK cell cytokine production or degranulation. Data are reported as % MIP1B+ cells of CD16+/CD56+ NK cells. **(C)** THP-1 monocyte cell line was used to measure antibody dependent cellular phagocytosis (ADCP), or the ability of antibody to induce phagocytosis of antigen. **(D)** Neutrophils isolated from donor blood were used to measure antibody dependent neutrophil phagocytosis (ADNP), or the ability of antibody to induce neutrophil phagocytosis of antigen. ADCP and ADNP are reported as a PhagoScore, calculated as (% bead positive monocytes/neutrophils) * (geometric MFI of each cell). **(E-H)** Pearson correlations between neutralizing antibody titers (Log_2NT50) and ADNP PhagoScores for are shown for: **(E)** ancestral, **(F)** BA.5, **(G)** XBB.1.5, and **(H)** JN.1 viruses. Separate R2 and p-values are shown for each virus separated by pregnancy status. **(A-E)** Data were analyzed by linear mixed effects regression analysis with Bonferroni post-hoc. Asterisks indicate $p < 0.05$.

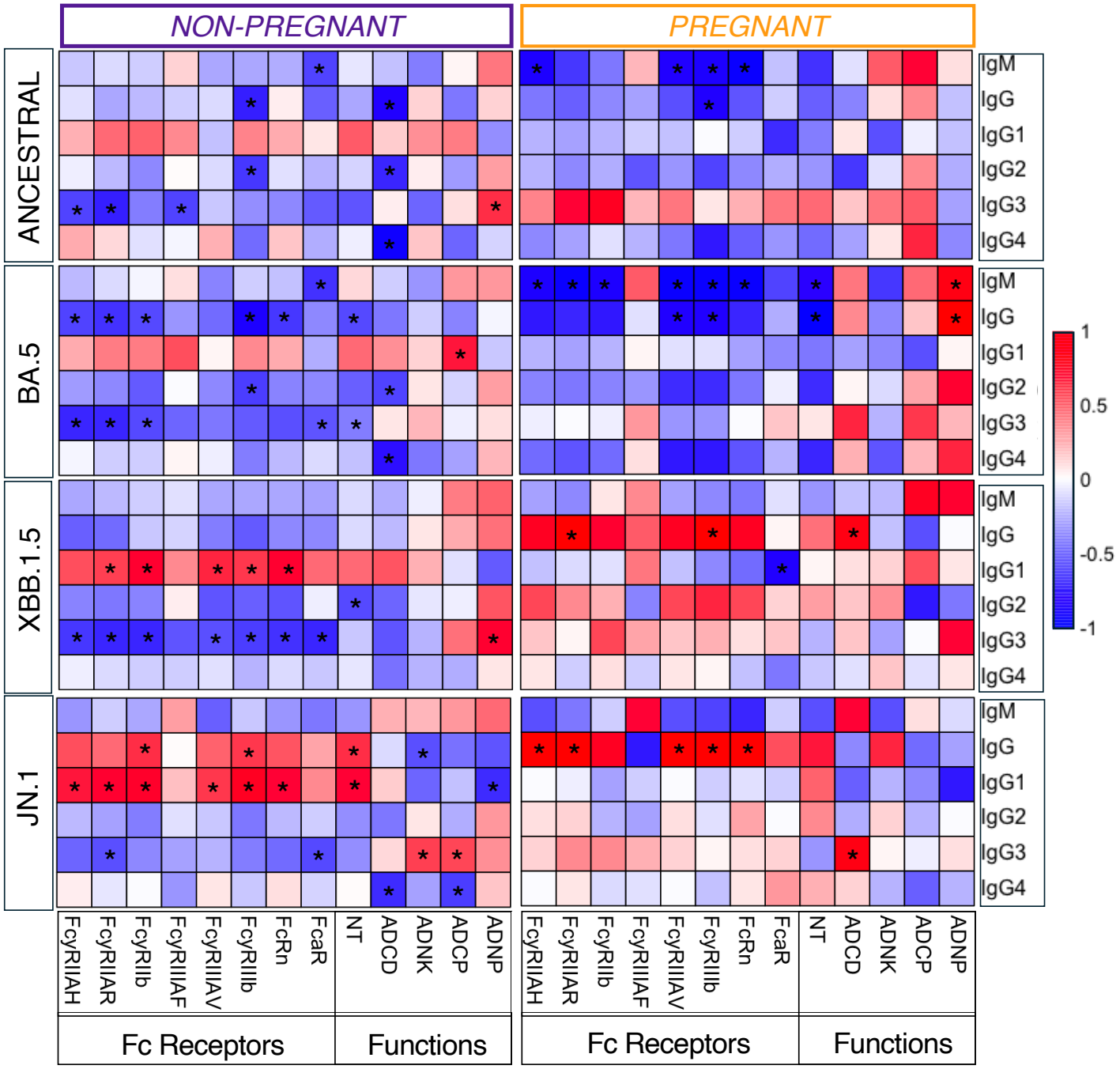

Figure 5. Correlations among IgG subclasses and antibody functional phenotypes differ between pregnant and nonpregnant individuals. Post-vaccination systems serology measures including isotype subclasses, FcR affinity, non-neutralizing functions, and neutralizing antibody (nAb) titers were $\log_{10}$ transformed and used for Spearman correlation analyses. Isotypes (y-axis) were correlated with functional measures (x-axis). Analyses were performed by pregnancy status. Asterisks indicate $p < 0.05$.

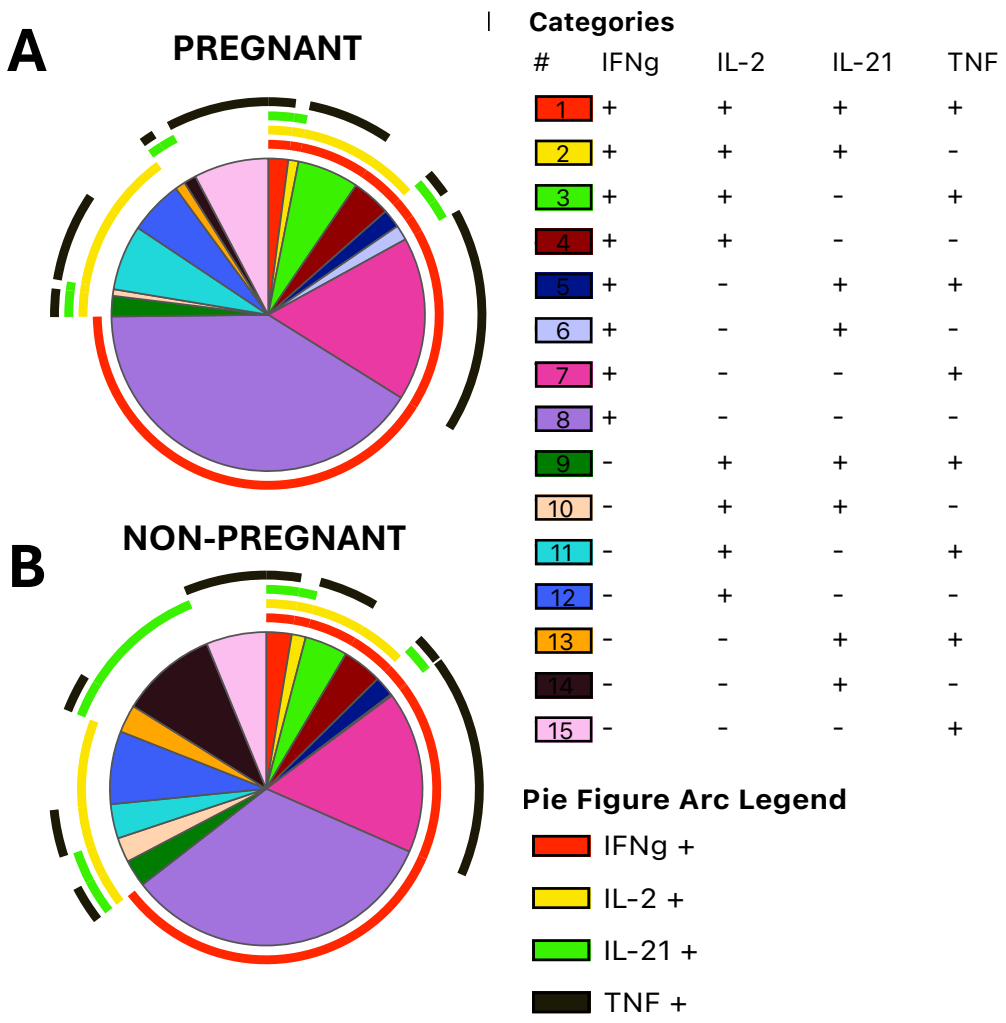

Figure 6. CD4+ T cells have reduced polyfunctionality among pregnant people. Peripheral blood mononuclear cells (PBMCs) were collected pre and 3-5 weeks post-vaccination for flow cytometry analyses. Cytokine-producing, antigen-specific CD4+T cells for **(A)** pregnant (n=7) and **(B)** non-pregnant (n=3) participants represented in pie charts broken down by the 15 cytokine combination categories. Arcs identify slices of the pie that express each specific cytokine**.** R values are shown for each correlation, and asterisks indicate $p < 0.05$.

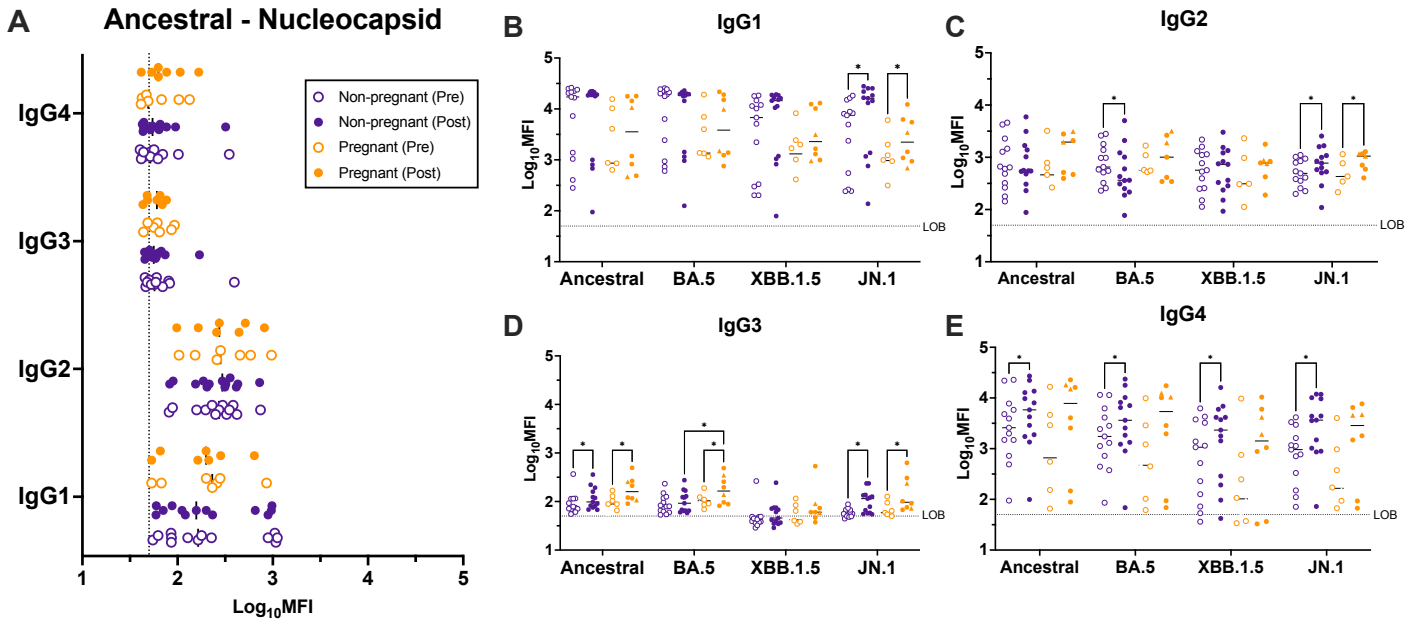

Supplemental Figure 1. Vaccination differently induces IgG subtype responses during pregnancy. IgG antibody responses in serum pre and 3-5 weeks post-vaccination were measured by systems serology and reported as $\log_{10}$ mean fluorescence intensity (MFI). Pregnant individuals (n=7) are shown in orange and non-pregnant females (n=13) in purple. Triangles highlight individuals who received monovalent boosters and circles represent bivalent booster recipients. **(A)** IgG subtype abundance to ancestral nucleocapsid (N) protein**.** IgG subtypes, including **(B)** IgG1 **(C)** IgG2, **(D)** IgG3, and **(E)** IgG4, in response to ancestral, BA.5, XBB.1.5, and JN.1 spike protein. Data were analyzed by linear mixed effects regression analysis with Bonferroni post-hoc. Asterisks indicate $p < 0.05$.

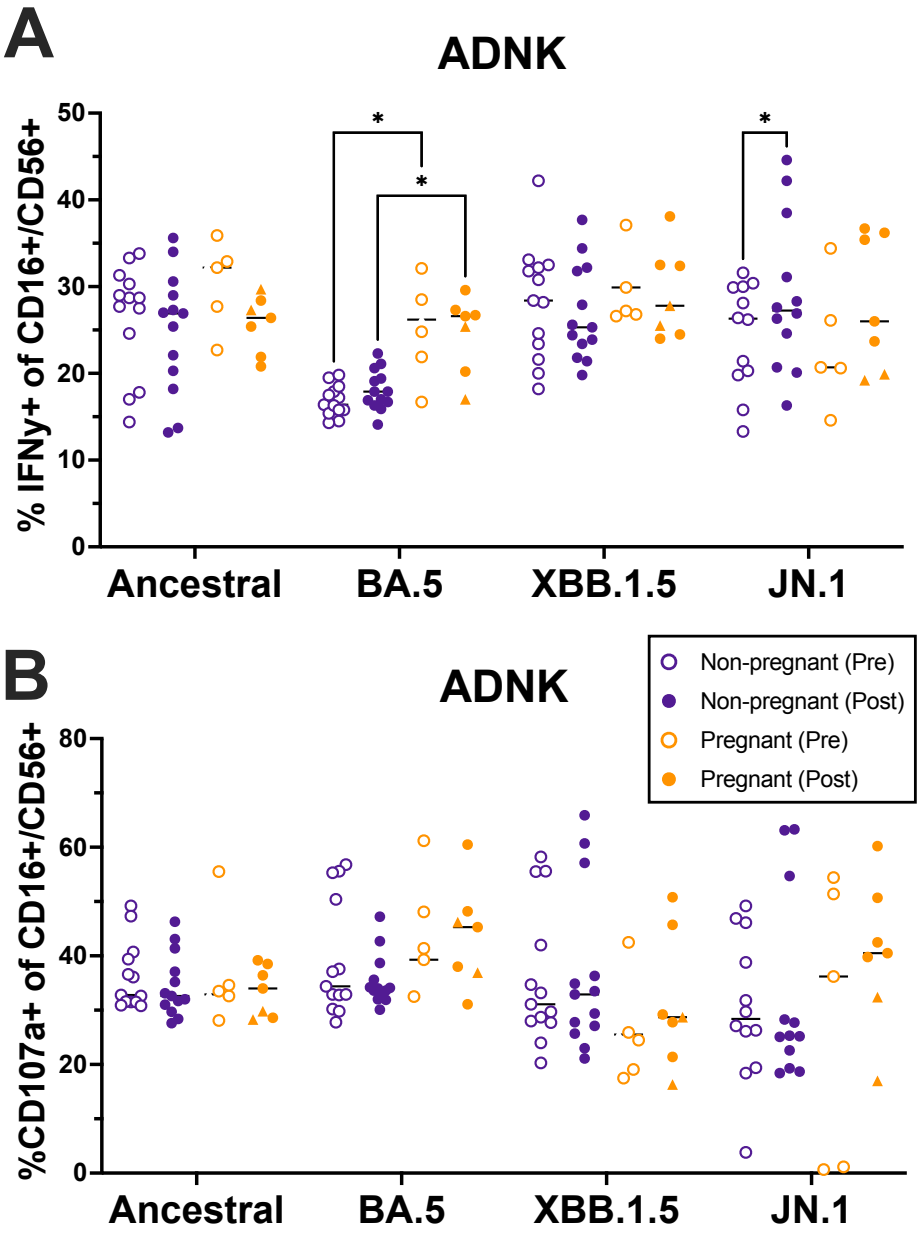

Supplemental Figure 2. Additional antibody-dependent NK cell responses by pregnancy status. NK cells isolated from donor blood were utilized to assess antibody dependent NK cell cytotoxicity (ADNK), or the ability of antigen specific serum antibody to include NK cell cytokine production or degranulation in serum pre and 3-5 weeks post-vaccination. Pregnant individuals (n=7) are shown in orange and non-pregnant females (n=13) in purple. Triangles highlight individuals who received monovalent boosters and circles represent bivalent booster recipients. ADNK was measured as ability to induce **(A)** IFNy production or **(B)** NK cell degranulation, as measured by CD107a positivity. Data were analyzed by linear mixed effects regression analysis with Bonferroni post-hoc. Asterisks indicate $p < 0.05$.

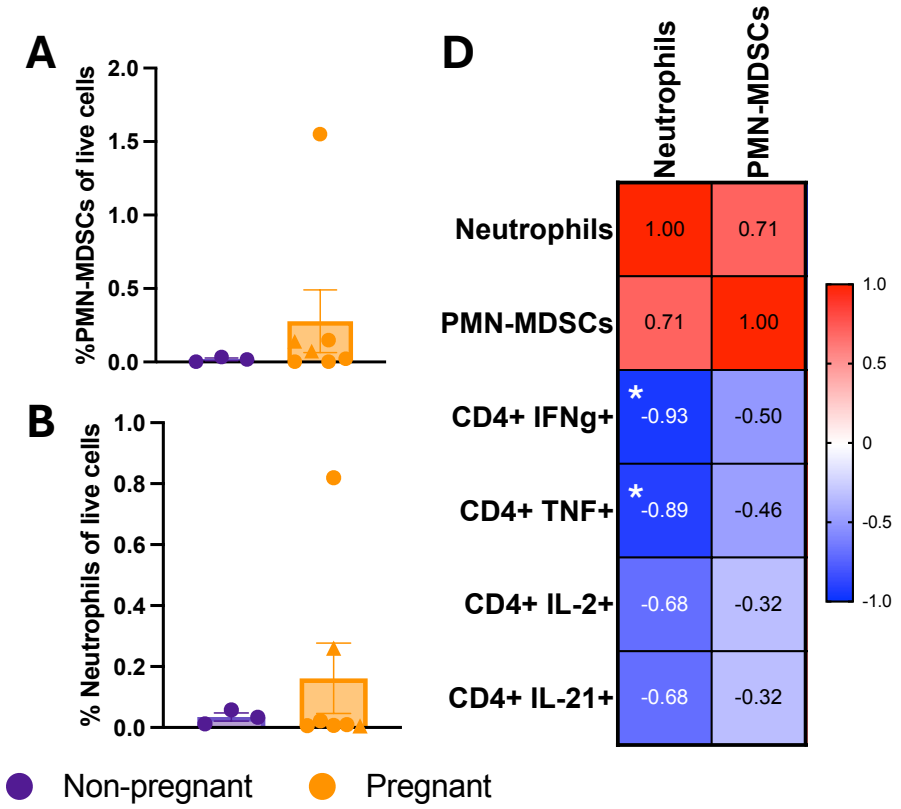

Supplemental Figure 3. Polymorphonuclear myeloid-derived suppressor cells correlate with CD4+ cytokine producing cells. Peripheral blood mononuclear cells (PBMCs) were collected pre and 3-5 weeks post-vaccination for flow cytometry analyses. Pregnant individuals (n=7) are shown in orange and non-pregnant females (n=3) in purple. Triangles highlight individuals who received monovalent boosters and circles represent bivalent booster recipients. **(A)** Neutrophils and **(C)** polymorphonuclear myeloid-derived suppressor cells (PMN-MDSCs) were quantified by flow cytometry and reported as a percentage of total live single cells. **(D)** Pearson correlations between cytokine producing CD4+ T cells, neutrophils, and PMN-MDSCs from pregnant people. R values are shown for each correlation, and asterisks indicate $p < 0.05$.

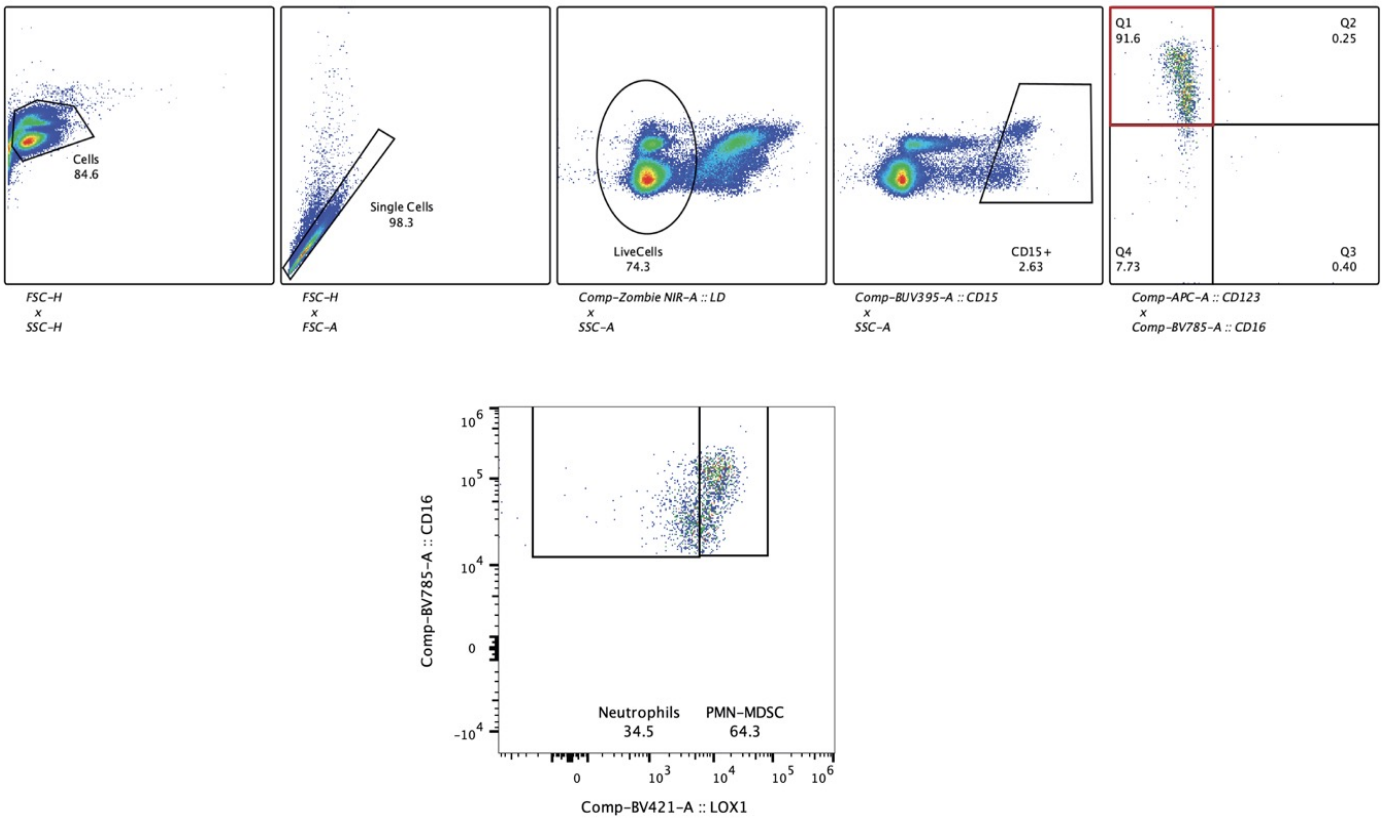

Supplemental Figure 4. PMN-MDSC gating strategy.

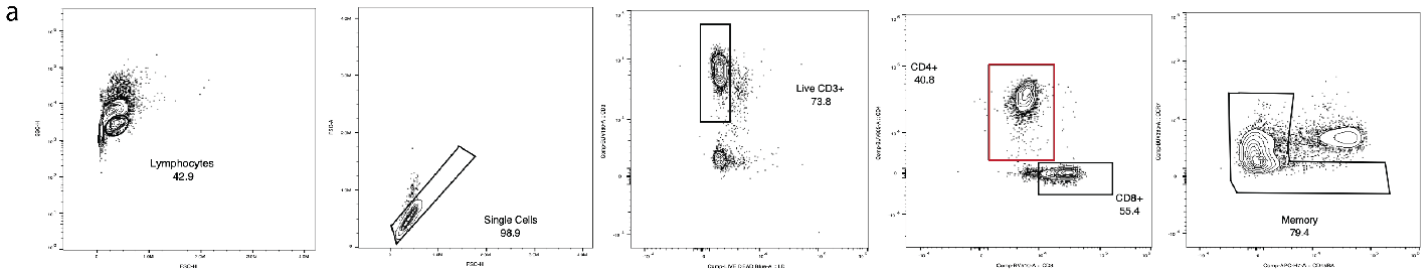

Supplemental Figure 5. Cytokine positive CD4+ T cells.

Supplemental Table 1A-B. Broad immune cell phenotyping (BIP) flow cytometry panel. (A) surface staining markers and **(B)** intracellular markers.

A. Surface

Fluorophore	Marker	Clone	Catalog	Vendor
BV570	CD33	WM53	303417	BioLegend
BV480	CD11c	B-ly6	566135	BD Biosciences
APC	CD123	6H6	306012	BioLegend
BV510	CD25	M-A251	563352	BD Biosciences
BV650	CCR7	G043H7	353234	BioLegend
BV421	LOX1	15C4	358610	BioLegend
BV711	CD38	HIT2	563965	BD Biosciences
APC-Cy7	CD19	SJ25C1	363010	BioLegend
APC-Cy7	CD56	5.1H11	362512	BioLegend
BV750	HLA-DR	L243	307672	BioLegend
BUV661	CD3	UCHT1	612964	BD Biosciences
BUV496	CD4	SK3	612936	BD Biosciences
BUV737	CD8	SK1	612754	BD Biosciences
BV785	CD16	3G8	302046	BioLegend
BUV805	CD14	M5E2	612902	BD Biosciences
BV605	CD86	BU63	374214	BioLegend
BUV563	CD45RA	HI100	612926	BD Biosciences
BUV395	CD15	H198	563872	BD Biosciences
Spark NIR	CD27	O232	302856	BioLegend
PE-Cy5	CD21	B-ly4	551064	BD Biosciences
PE-Cy5.5*	CD138	MI15	356502	BioLegend
PE-CF594	KLRG1	2F1	565393	BD Biosciences
BB790	IgD	IA6-2	BD Custom	BD Biosciences
BUV615	PD-1	EH12.1	612991	BD Biosciences

B. Intracellular

Fluorophore	Marker	Clone	Catalog	Vendor
Pacific Blue	FOXP3	206D	320116	BioLegend
PE-Cy7	Ki-67	Ki-67	350526	BioLegend
Alexa Fluor 488	CPT1a	8F6AE9	ab171449	Abcam
Alexa Fluor 680**	HK2	EPR20839	ab228819	Abcam
Alexa Fluor 532***	VDAC1	20B12AF2	ab14734	Abcam

Alexa Fluor 405	Tomm20	EPR15581-54	ab210047	Abcam
Alexa Fluor 647	GLUT1	EPR3915	ab195020	Abcam

Notes: * conjugated using PE/Cy5.5 Conjugation Kit - Lightning-Link (ab102899)

** conjugated using DyLight 680 Conjugation Kit (Fast) - Lightning-Link (ab201804)

*** conjugated using Alexa Fluor 532 Antibody Labeling Kit (Thermo Fisher, A20182)

Supplemental Table 2. Intracellular cytokine staining (ICS) flow cytometry panel. (A) surface staining markers and **(B)** intracellular markers.

A. Surface

Fluorophore	Marker	Clone	Catalog	Vendor
BUV395	CCR7	2-L1-A	749655	BD Biosciences
BV650	CXCR3	1C6	740603	BD Biosciences
PE CF594	KLRG1	2F1	565393	BD Biosciences
BV605	CD69	FN50	562989	BD Biosciences
BUV563	CD25	2A3	612918	BD Biosciences
BUV661	PD-1	EH12.1	750260	BD Biosciences
BUV737	TIM-3	7D3	748820	BD Biosciences
BV570	CD28	CD28.2	302926	Biolegend
PE Cy5	CD127	HIL-7R-M21	BD Custom	BD Biosciences
BUV805	CD4	SK3	612887	BD Biosciences
APC H7	CD45RA	HI100	560674	BD Biosciences
BB660	Tigit	741182	BD Custom	BD Biosciences
BV711	OX40	ACT35	563664	BD Biosciences
BV786	CD27	L128	563327	BD Biosciences
PE Cy7	CTLA-4	BNI3	BD Custom	BD Biosciences
BV510	CD8a	HIT8a	300934	Biolegend
BB790	CXCR5	RF8B2	BD Custom	BD Biosciences

B. Intracellular

Fluorophore	Marker	Clone	Catalog	Vendor
PE	IL-21	3A3-N2	513004	BioLegend
AF680**	HK2	EPR20839	ab228819	Abcam
AF488	TCF1	812145	IC8224G	FisherScientific
BV421	IL-2	MQ1-17H12	564164	BD Biosciences
AF532***	VDAC1	20B12AF2	ab14734	Abcam

BV750	TNF	MAb11	566359	BD Biosciences
PECy5.5*	CPT1a	8F6AE9	ab128568	Abcam
AF405	Tomm20	EPR15581-54	ab210047	Abcam
Alexa647	GLUT1	EPR3915	ab195020	Abcam
BUV496	CD3	UCHT1	612940	BD Biosciences
BB700	IFNy	B27	566394	BD Biosciences

Notes: * conjugated using PE/Cy5.5 Conjugation Kit - Lightning-Link (ab102899)

** conjugated using DyLight 680 Conjugation Kit (Fast) - Lightning-Link (ab201804)

*** conjugated using Alexa Fluor 532 Antibody Labeling Kit (Thermo Fisher, A20182)